

**20 new
Experiments**



PHYSICS & ENGINEERING EXPERIMENTS

3bscientific.com

Mechanics · Heat · Electricity · Optics · Atomic and Nuclear Physics · Physics of Solid Bodies · Energy and Environment

Dear Customers,

Are you familiar with the 3B Scientific® catalogue, which features more than 110 experiments? It is still right up to date and includes a fascinating selection of experiments. The assortment covers the entire spectrum of physics ranging from classical to modern. We are delighted to announce the introduction of 20 brand new experiments.

Particular highlights are experiments on the following subjects:

- Elastic deformation of solid bodies (modulus of elasticity, shear modulus)
- Propagation of sound in rods
- Investigation of Pockels effect
- Determination of elementary charge by means of Millikan's experiment
- Installation and optimisation of photovoltaic systems

If you require sets of apparatus for other topics, we can gladly assemble them for you on request. That means we can be even more specific in giving you what you need. You can contact us by telephone, e-mail or via our website 3bscientific.com. We look forward to any suggestions, queries or orders.

All the experiments are available to download from our website in PDF format. You will always find plenty of new equipment sets there too.



Prism Spectrometer, Page 32

Committed to quality

3B Scientific provides you with good quality at fair prices. Our sophisticated quality management complies with the ISO 9001 standards and the Worlddidac Quality Charter and is regularly approved by independent experts.

That's something you can rely on.



LEGEND



Basic experiment



Intermediate experiment



Look for more Experiments at 3bscientific.com

CONTENT

MECHANICS

FORCES

Hooke's Law (UE1020100):	4
Confirm Hooke's law for coil springs under tension	

TRANSLATIONAL MOTION

Laws of Collisions (UE1030280):	6
Investigate uni-dimensional collisions on an air track	

ROTATIONAL MOTION

Maxwell's Wheel (UE1040320):	8
Confirm the conservation of energy with the help of Maxwell's wheel	

OSCILLATIONS

Kater's Reversible Pendulum (UE1050221):	10
Work out the local acceleration due to gravity with the help of a reversible pendulum	

ACOUSTICS

Propagation of Sound in Rods (UE1070410):	12
Investigation of longitudinal sound waves in cylindrical rods and determination of propagation velocity for longitudinal sound waves	

DEFORMATION OF SOLID BODIES

Bending of Flat Beams (UE1090200):	14
Measurement of deformation of flat beams supported at both ends and determination of modulus of elasticity	
Torsion on Cylindrical Rods (UE1090300):	16
Determination of torsional coefficients and shear modulus	

HEAT

GAS LAWS

Amontons' Law (UE2040120):	18
Verify the linear relationship between the pressure and temperature of an ideal gas	

ELECTRICITY

MAGNETIC FIELDS

Electric Balance (UE3030350):	20
Measurement of the force exerted on a current-carrying conductor located inside a magnetic field	

INDUCTION

Induction Through a Varying Magnetic Field (UE3040300):	22
Measuring the voltage induced in an induction coil	

OPTICS

GEOMETRIC OPTICS

Reflection in a Mirror (UE4010000):	24
Investigate reflection from a plane mirror and a curved mirror	
Refraction of Light (UE4010020):	26
Investigate refraction of light by various optical components	

WAVE OPTICS

Diffraction by a Single Slit (UE4030100):	28
Demonstrate the wave nature of light and determine the wavelength	

POLARISATION

Pockels Effect (UE4040500):	30
Demonstration of Pockels effect in a conoscopic beam path	

SPECTROMETRY

Prism Spectrometer (UE4080100):	32
Set up and calibrate a prism spectrometer	

ATOMIC AND NUCLEAR PHYSICS

INTRODUCTORY EXPERIMENTS IN ATOMIC PHYSICS

Millikan's Experiment (UE5010400):	34
Carry out Millikan's experiment to confirm the value of the elementary charge with the help of charged oil drops	

PHYSICS OF SOLID BODIES

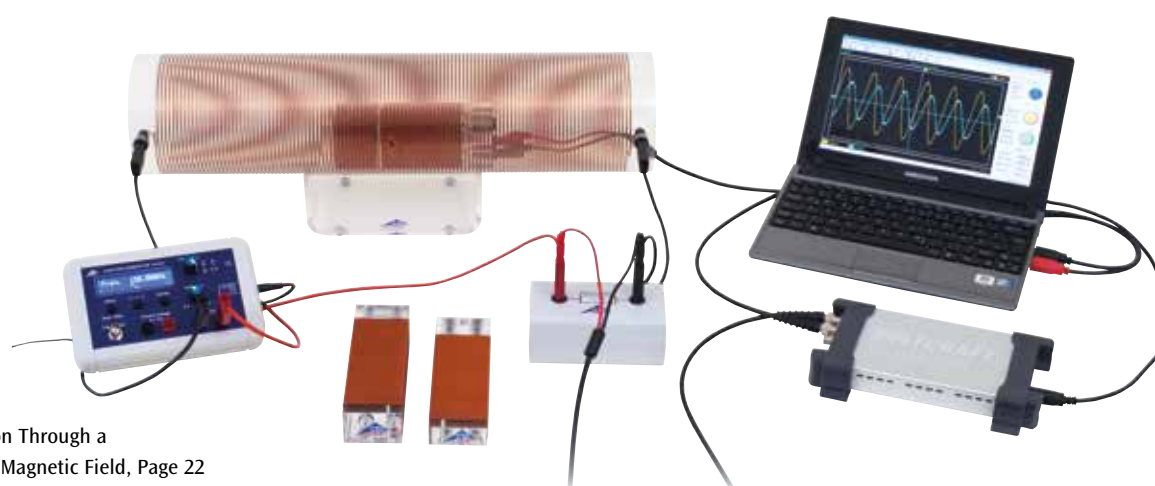
CONDUCTION PHENOMENA

Photoconductivity (UE6020400):	36
Record the characteristic curve for a photoresistor	

ENERGY AND ENVIRONMENT

PHOTOVOLTAICS

Photovoltaic Systems (UE8020100):	38
Record the characteristics of a photovoltaic module (solar cell) as a function of the luminosity	
Photovoltaic Systems (UE8020200):	40
Investigate how partial shading affects photovoltaic systems	
Photovoltaic Systems (UE8020250):	42
Investigation of an island grid or microgrid used to generate and store electrical energy	



Induction Through a Varying Magnetic Field, Page 22

**OBJECTIVE**

Confirm Hooke's law for coil springs under tension

EXPERIMENT PROCEDURE

- Confirm Hooke's law and determine the spring constant of five different coil springs.
- Compare the measured spring constants with those calculated theoretically.



You can find technical information about the equipment at 3bscientific.com

1

SUMMARY

In any elastic body, extension and tension are proportional to one another. This relationship was discovered by *Robert Hooke* and is frequently demonstrated using a coil spring with weights suspended from it. The change in the length of the spring is proportional to the force of gravity F on the suspended weight. In this experiment, five different coil springs will be measured. Thanks to a suitable choice of wire diameter and coil diameter, the spring constants all span one order of magnitude. In each case, the validity of Hooke's law will be demonstrated for forces in excess of the initial tension.

REQUIRED APPARATUS

Quantity	Description	Number
1	Set of Helical Springs for Hooke's Law	1003376
1	Set of Slotted Weights, 20 – 100 g	1003226
1	Vertical Ruler, 1 m	1000743
1	Set of Riders for Rulers	1006494
1	Barrel Foot, 1000 g	1002834
1	Stainless Steel Rod 1000 mm	1002936
1	Tripod Stand 150 mm	1002835
1	Clamp with hook	1002828
Additionally recommended		
1	Callipers, 150 mm	1002601
1	External Micrometer	1002600

BASIC PRINCIPLES

In any elastic body, extension and tension are proportional to one another. This relationship was discovered by *Robert Hooke* and is a good description of how a large number of materials behave when the degree of deformation is sufficiently small. This law is frequently demonstrated using a coil spring with weights suspended from it. The change in the length of the spring is proportional to the force of gravity F on the suspended weight.

For the sake of greater precision, it is first necessary to determine the initial tension which may be exhibited by the spring as the result of its manufacturing process. It is necessary to compensate for this by adding a weight which applies a force F_1 , causing the spring to extend from its natural length without any weight s_0 to a length s_1 . For weights in excess of F_1 , Hooke's law applies in the following form:

$$(1) \quad F - F_1 = k \cdot (s - s_1),$$

This is so as long as the length of the spring s does not exceed a certain critical length.

The spring constant k depends on the material and the geometric dimensions of the spring. For a cylindrical coil spring with n turns of constant diameter D , the following is true:

$$(2) \quad k = G \cdot \frac{d^4}{D^3} \cdot \frac{1}{8 \cdot n}.$$

d : Diameter of wire coils of spring

The shear modulus G for the steel wire forming the spring's coils is 81.5 GPa.

In this experiment, five different coil springs will be measured. Thanks to a suitable choice of wire diameter and coil diameter, the spring constants all span one order of magnitude. In each case, the validity of Hooke's law will be demonstrated for forces in excess of the initial tension.

EVALUATION

The force of gravity F can be determined to sufficient precision from the mass m of the weight as follows:

$$F = m \cdot 10 \frac{\text{m}}{\text{s}^2}$$

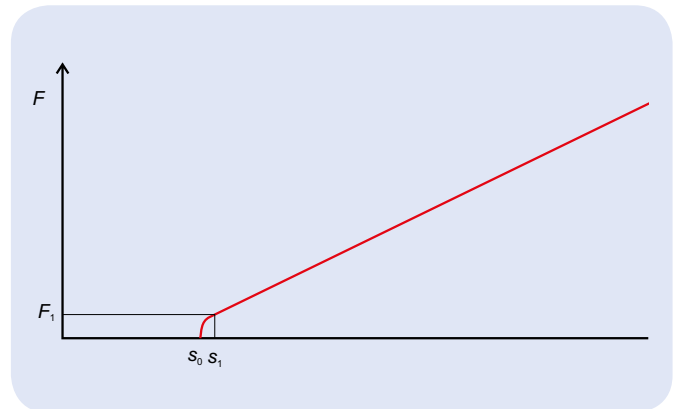


Fig. 1: Schematic of characteristic curve for a spring coil of length s with a certain initial tension

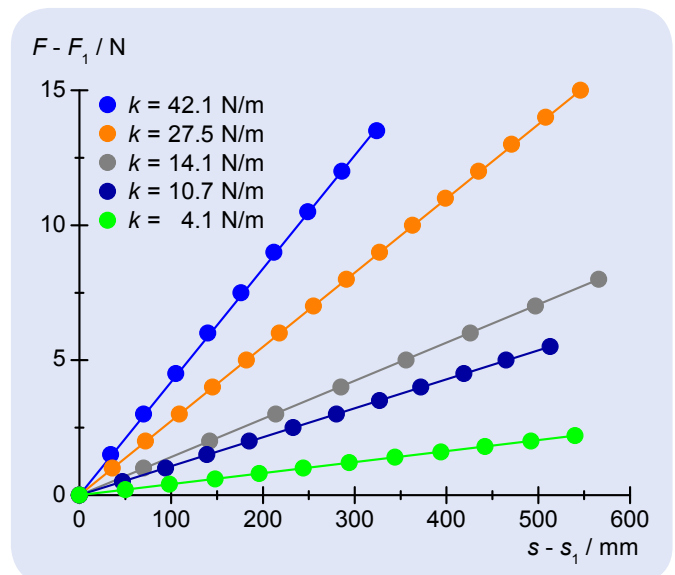
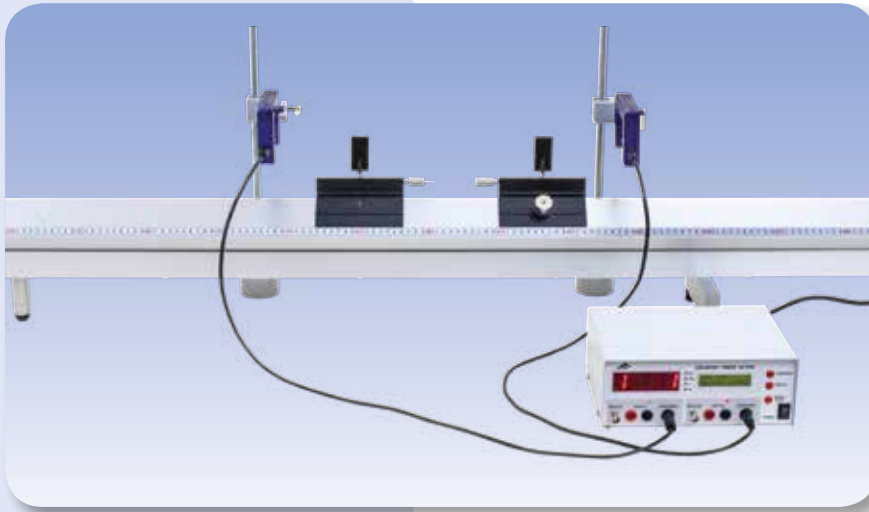


Fig. 2: Load as a function of the change in length

**OBJECTIVE**

Investigate uni-dimensional collisions on an air track

SUMMARY

One important consequence of Newton's third law is the conservation of momentum in collisions between two bodies. One way of verifying this is to investigate collisions between two sliders on an air track. When all of the kinetic energy is conserved, we speak of elastic collisions. In cases where kinetic energy is only conserved for the common centre of gravity of the two bodies, we use the term inelastic collisions.

In this experiment, the individual velocities of the sliders are determined from the times that photoelectric light barriers are interrupted and the momentum values are calculated from these speeds.

EXPERIMENT PROCEDURE

- Investigate elastic and inelastic collisions between two sliders on an air track.
- Demonstrate conservation of momentum for elastic and inelastic collisions and observe the individual momenta for elastic collisions.
- Investigate how energy is distributed in elastic and inelastic collisions.

REQUIRED APPARATUS

Quantity	Description	Number
1	Air Track	1019299
1	Air Flow Generator (230 V, 50/60 Hz)	1000606 or
	Air Flow Generator (115 V, 50/60 Hz)	1000605
1	Digital Counter with Interface (230 V, 50/60 Hz)	1003123 or
	Digital Counter with Interface (115 V, 50/60 Hz)	1003122
2	Photo Gate	1000563
2	Barrel Foot, 1000 g	1002834
2	Universal Clamp	1002830
2	Stainless Steel Rod 470 mm	1002934
Additionally recommended		
1	Mechanical Balance 610	1003419

BASIC PRINCIPLES

One important consequence of Newton's third law is the conservation of momentum in collisions between two bodies. One way of verifying this is to investigate collisions between two sliders on an air track.

In the frame of reference of their common centre of gravity, the total momentum of two bodies of masses m_1 and m_2 is zero both before and after the collision.

$$(1) \quad \vec{p}_1 + \vec{p}_2 = \vec{p}'_1 + \vec{p}'_2 = 0$$

\vec{p}_1, \vec{p}_2 : Individual momenta before collision, \vec{p}'_1, \vec{p}'_2 : Individual momenta after collision

The kinetic energy of the two sliders in the same frame of reference is given by

$$(2) \quad \vec{E} = \frac{\vec{p}_1^2}{2m_1} + \frac{\vec{p}_2^2}{2m_2}$$

Depending on the nature of the collision, this may be converted partially or even wholly into other forms of energy. When all of the kinetic energy is conserved in frame of reference of the common centre of gravity, we speak of elastic collisions. In an inelastic collision, all the energy is converted into another form.



You can find technical information about the equipment at 3bscientific.com

Using the track itself as the frame of reference, conservation of momentum is described by the following equation:

$$(3) \quad p_1 + p_2 = p'_1 + p'_2 = p = \text{const.}$$

p_1, p_2 : Individual momenta before collision
 p'_1, p'_2 : Individual momenta after collision

As a result of conservation of momentum, the velocity of the centre of gravity

$$(4) \quad v_c = \frac{p}{m_1 + m_2}$$

and its kinetic energy

$$(5) \quad E_c = \frac{m_1 + m_2}{2} \cdot v_c^2$$

are also conserved. This is true of both elastic and inelastic collisions. In this experiment, the second slider is initially at rest before the collision. Therefore the conservation of momentum (equation 3) is given by

$$(6) \quad p = m_1 \cdot v_1 = m_1 \cdot v'_1 + m_2 \cdot v'_2$$

Here v'_1 and v'_2 have different values after an elastic collision, but are the same subsequent to an inelastic collision. In an elastic collision, a flat buffer on the first slider collides with a stretched rubber band on the second slider. An inelastic collision involves a long pointed spike being pushed into some modelling clay. The masses of the sliders can be modified by adding weights.

After an elastic collision the following relationships apply:

$$(7) \quad p'_1 = \frac{m_1 - m_2}{m_1 + m_2} \cdot p, \quad p'_2 = \frac{2 \cdot m_2}{m_1 + m_2} \cdot p$$

and

$$(8) \quad E = \frac{m_1}{2} \cdot v_1^2 = \frac{m_1}{2} \cdot v_1'^2 + \frac{m_2}{2} \cdot v_2'^2$$

In the case of an inelastic collision only the kinetic energy of the centre of gravity remains conserved. This can be calculated using equations (4), (5) and (6)

$$(9) \quad E_c = \frac{m_1}{m_1 + m_2} \cdot \frac{m_1}{2} \cdot v_1^2 = \frac{m_1}{m_1 + m_2} \cdot E$$

EVALUATION

The time intervals Δt saved by the digital counter are to be matched with experimental procedures. The following applies to the velocities of the sliders

$$v = \frac{25 \text{ mm}}{\Delta t}$$

If no weighing scales are available, it may be assumed that the mass of a slider is 204 g. The mass of all the weights together is 200 g. A precise consideration of the velocity and momentum distributions should also take into account frictional losses. For the momentum values obtained here, they should amount to some 5% and for the energy values 10%, see Figs. 1 to 5.

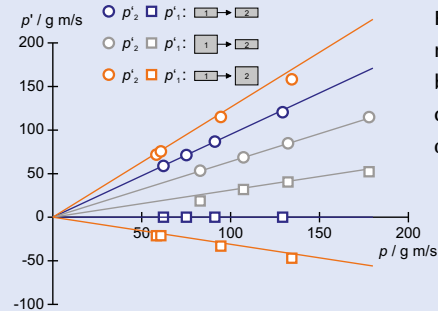


Fig. 1: Individual momenta for colliding bodies after an elastic collision as a function of initial momentum

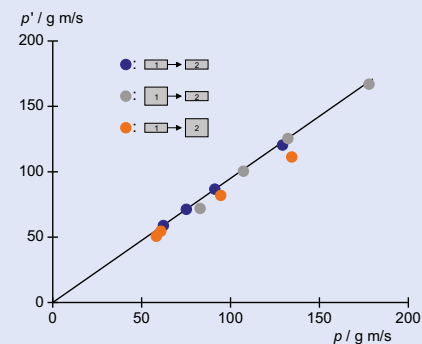


Fig. 2: Total momentum for colliding bodies after an elastic collision as a function of initial momentum

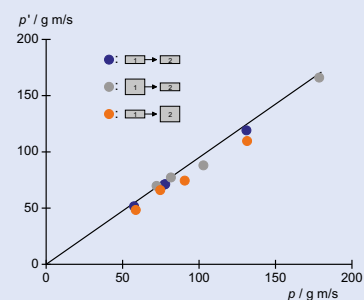


Fig. 3: Total momentum for colliding bodies after an inelastic collision as a function of initial momentum

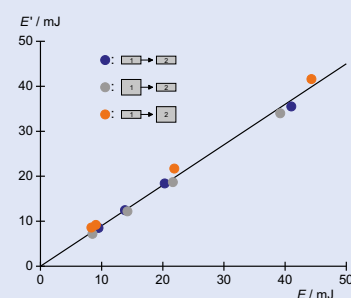


Fig. 4: Total energy for colliding bodies after an elastic collision as a function of initial energy

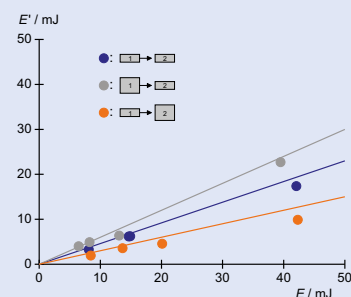
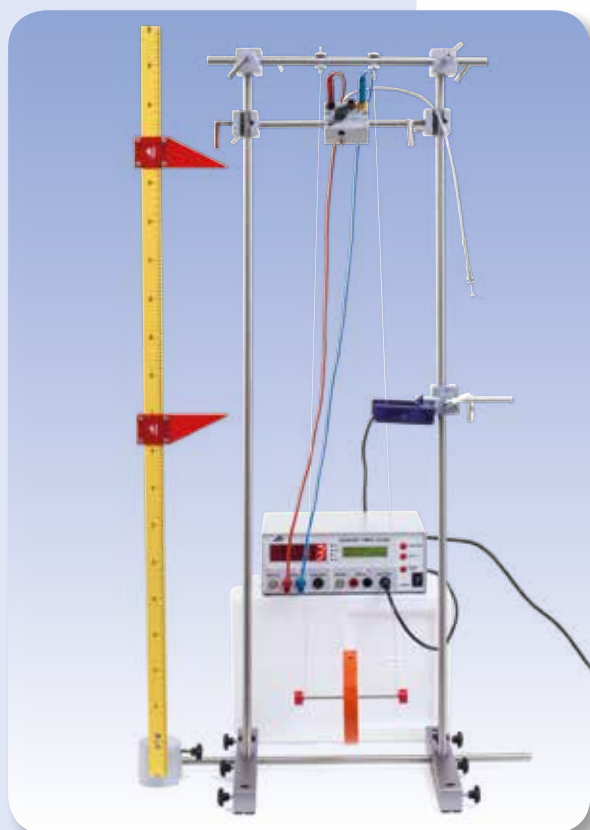


Fig. 5: Total energy for colliding bodies after an inelastic collision as a function of initial energy

UE1040320

MAXWELL'S WHEEL



OBJECTIVE

Confirm the conservation of energy with the help of Maxwell's wheel

SUMMARY

Maxwell's wheel is suspended from threads at both ends of its axle in such a way that it can roll along the threads. In the course of its motion, potential energy is converted into kinetic energy and back again. The process of rolling up and down is repeated until the potential energy derived from the initial height of the wheel is entirely lost due to reflection losses and friction. In this experiment a photo-electric light barrier is set up at various different heights in such a way that the axle of Maxwell's wheel repeatedly breaks the beam. From the times between these interruptions of the beam it is possible to establish the instantaneous speed of the wheel and thereby to calculate its kinetic energy.

EXPERIMENT PROCEDURE

- Plot a graph of displacement against time and another of speed against time for the first downward roll.
- Determine the acceleration and the moment of inertia.
- Determine the kinetic energy and potential energy during upward and downward motions.
- Confirm the conservation of energy taking into account losses due to reflection and friction.



You can find technical information about the equipment at 3bscientific.com

1

REQUIRED APPARATUS

Quantity	Description	Number
1	Maxwell's Wheel	1000790
1	Trigger Device for Maxwell's Wheel	1018075
1	Digital Counter with Interface (230 V, 50/60 Hz)	1003123 or
	Digital Counter with Interface (115 V, 50/60 Hz)	1003122
1	Photo Gate	1000563
1	Stand with H-Shaped Base	1018874
2	Stainless Steel Rod 1000 mm	1002936
5	Universal Clamp	1002830
1	Stainless Steel Rod, 400 mm, 10 mm diam.	1012847
1	Pair of Safety Experimental Leads, 75 cm, red/blue	1017718
Additionally recommended		
1	Electronic Scale 5000 g	1003434
1	Callipers, 150 mm	1002601

BASIC PRINCIPLES

Maxwell's wheel is suspended from threads at both ends of its axle in such a way that it can roll along the threads. As it moves, potential energy is increasingly converted into kinetic energy of the spinning wheel. Once the threads are fully wound out, though, they then start to wind up the opposite way round and the wheel rises, whereby the kinetic energy is converted back into potential energy until all of it is reconverted. The wheel then keeps rolling down and back up again until the potential energy derived from the initial height of the wheel is entirely lost due to reflection losses and friction.

As it rolls up and down, the wheel moves at a velocity v . The velocity obeys the following fixed relationship to the angular velocity ω with which the wheel rotates about its axle:

$$(1) \quad v = \omega \cdot r \text{ where } r = \text{radius of axle.}$$

The total energy is therefore given by

$$(2) \quad E = m \cdot g \cdot h + \frac{1}{2} \cdot I \cdot \omega^2 + \frac{1}{2} \cdot m \cdot v^2 \\ = m \cdot g \cdot h + \frac{1}{2} \cdot m \cdot \left(\frac{I}{m \cdot r^2} + 1 \right) \cdot v^2$$

m : mass, I : moment of inertia,

h : height above lower point of reversal, g : acceleration due to gravity

This describes a translational motion with an acceleration downwards given by

$$(3) \quad \dot{v} = a = \frac{g}{\frac{I}{m \cdot r^2} + 1}$$

This acceleration is determined in the experiment from the distance covered in time t

$$(4) \quad s = \frac{1}{2} \cdot a \cdot t^2.$$

It can also be determined from the instantaneous speed attained after a time t

$$(5) \quad v = a \cdot t.$$

The measurement involves setting up a photo-electric light barrier at various heights h , whereby the light beam is repeatedly broken by the axle of the wheel as it rolls up and down (see Fig. 1). A digital counter measures the time between interruptions of the beam Δt and the time t it takes the wheel to descend in its initial downward roll.

EVALUATION

If the mass of the wheel m and the radius of its axle r are known, the moment of inertia can be determined from the acceleration a . From equation (3), the following must be true:

$$I = m \cdot r^2 \cdot \left(\frac{g}{a} - 1 \right).$$

The instantaneous speeds v and kinetic energies E_{kin} are calculated from the intervals between interruptions Δt as follows:

$$v = \frac{2 \cdot r}{\Delta t} \quad \text{and} \quad E_{\text{kin}} = \frac{1}{2} \cdot m \cdot \left(\frac{I}{m \cdot r^2} + 1 \right) \cdot v^2.$$

The potential energy is given by

$$E_{\text{pot}} = m \cdot g \cdot h.$$

The energy losses which are clearly apparent from Fig. 4 are described quite well by assuming a constant force of friction acting in opposition to the direction of motion and an appreciable loss of energy when the direction changes at the bottom of the motion.

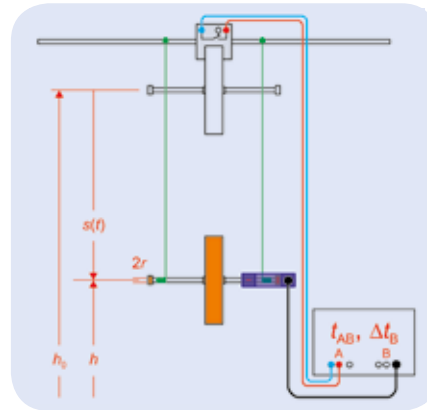


Fig. 1: Schematic of experiment set-up

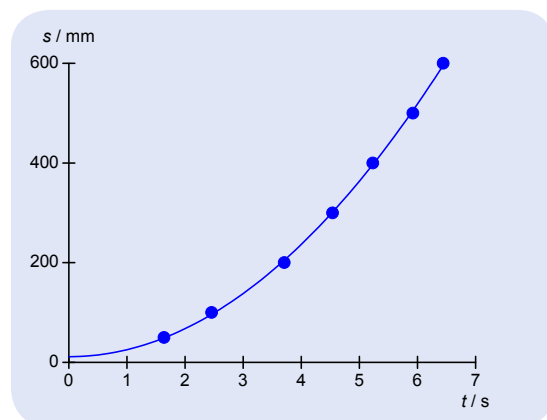


Fig. 2: Graph of displacement against time for initial downward motion

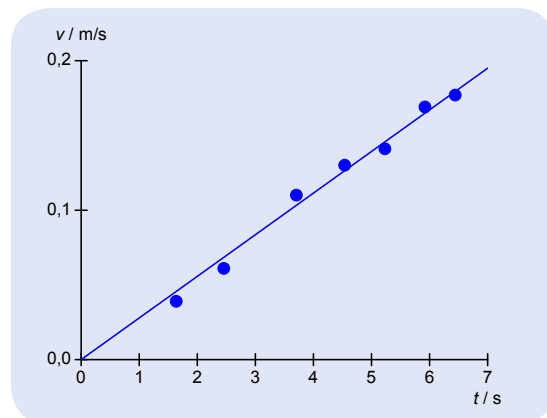


Fig. 3: Graph of speed against time for initial downward motion

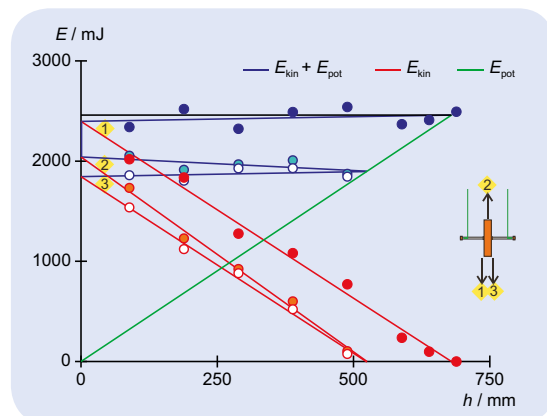


Fig. 4: Energy distribution as a function of height h

**OBJECTIVE**

Work out the local acceleration due to gravity with the help of a reversible pendulum

EXPERIMENT PROCEDURE

- **Configure a reversible pendulum such that the periods of oscillation are the same from both mounting points.**
- **Determine the period of oscillation and calculate the local acceleration due to gravity.**



You can find technical information about the equipment at 3bscientific.com

1

SUMMARY

A reversible pendulum is a special design of a normal physical pendulum. It is able to swing from either of two mounting points and can be set up in such a way that the period of oscillation is the same from both these points. The reduction in the length of the pendulum then matches the distance between the two mounting points. This makes it easier to determine the local acceleration due to gravity from the period of oscillation and the reduced pendulum length. Matching of the reversing pendulum is achieved by moving a weight between the mounts as appropriate while a rather larger counterweight outside that length remains fixed.

REQUIRED APPARATUS

Quantity	Description	Number
1	Kater's Reversible Pendulum	1018466
1	Photo Gate	1000563
1	Digital Counter (230 V, 50/60 Hz)	1001033 or
	Digital Counter (115 V, 50/60 Hz)	1001032

BASIC PRINCIPLES

A reversible pendulum is a special design of a normal physical pendulum. It is able to swing from either of two mounting points and can be set up in such a way that the period of oscillation is the same from both these points. The reduction in the length of the pendulum then matches the distance between the two mounting points. This makes it easier to determine the local acceleration due to gravity from the period of oscillation and the reduced pendulum length.

If a physical pendulum oscillates freely about its rest position with a small deflection ϕ then its equation of motion is as follows:

$$(1) \quad \frac{J}{m \cdot s} \cdot \ddot{\phi} + g \cdot \phi = 0.$$

J : Moment of inertia about axis of oscillation,
 g : Acceleration due to gravity, m : Mass of pendulum,
 s : Distance between axis of oscillation and centre of gravity

The reduced length of the physical pendulum is

$$(2) \quad L = \frac{J}{m \cdot s}$$

A mathematical pendulum of this length oscillates with the same period of oscillation.

Steiner's law gives us the moment of inertia:

$$(3) \quad J = J_s + m \cdot s^2$$

J_s : Moment of inertia about centre of gravity axis

For a reversible pendulum with two mounting points separated by a distance d , the reduced lengths to be assigned are therefore

$$(4) \quad L_1 = \frac{J_s}{m \cdot s} + s \quad \text{and} \quad L_2 = \frac{J_s}{m \cdot (d - s)} + d - s$$

They match up if the reversible pendulum is configured in such a way that the period of oscillation is the same for both mounting points. In that case, the following is true:

$$(5) \quad s = \frac{d}{2} \pm \sqrt{\left(\frac{d}{2}\right)^2 - \frac{J_s}{m}}$$

and

$$(6) \quad L_1 = L_2 = d.$$

In this case, the period of oscillation T is given by

$$(7) \quad T = 2\pi \cdot \sqrt{\frac{d}{g}}$$

In the experiment, matching of the reversible pendulum is accomplished by moving a weight of mass $m_2 = 1$ kg between the mounting points as appropriate. A second large counterweight of mass $m_1 = 1.4$ kg is fixed outside the mounts. Measurement of the period of oscillation is handled electronically with the lower end of the pendulum periodically interrupting a photoelectric gate. By this means, the periods of oscillation T_1 and T_2 associated with the reduced pendulum lengths L_1 and L_2 are measured as a function of the position x_2 of weight m_2 .

EVALUATION

The two curves derived from the measurements $T_1(x_2)$ and $T_2(x_2)$ intersect twice at the value $T = T_1 = T_2$. To determine the intersects accurately requires interpolation between the measurement points themselves. Acceleration due to gravity is calculated from the measurements as follows:

$$g = \left(\frac{2\pi}{T}\right)^2 \cdot d, \quad d = 0.8 \text{ m}$$

with relative precision of 0.3 per thousand.

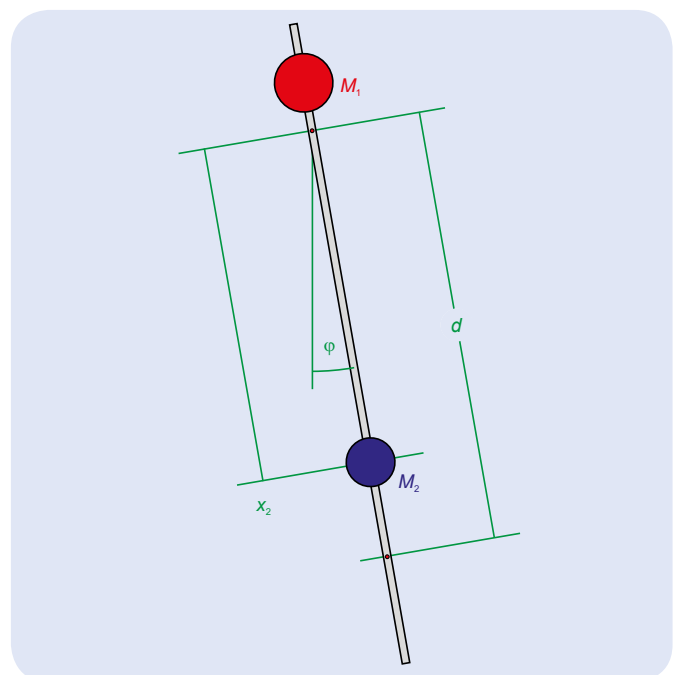


Fig. 1: Schematic diagram of a reversible pendulum

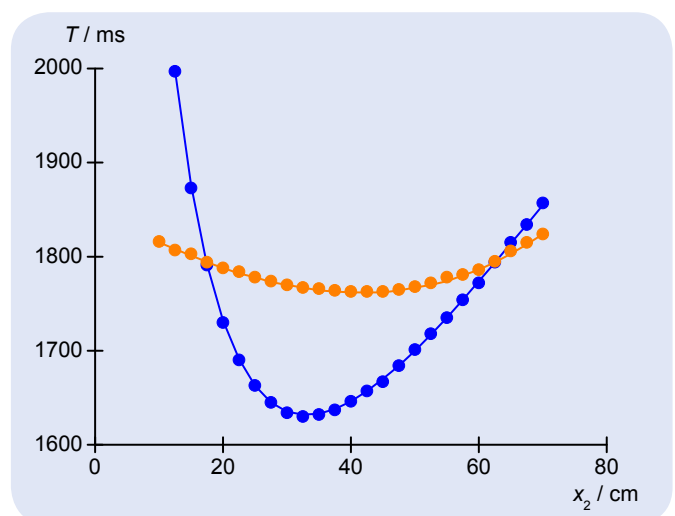
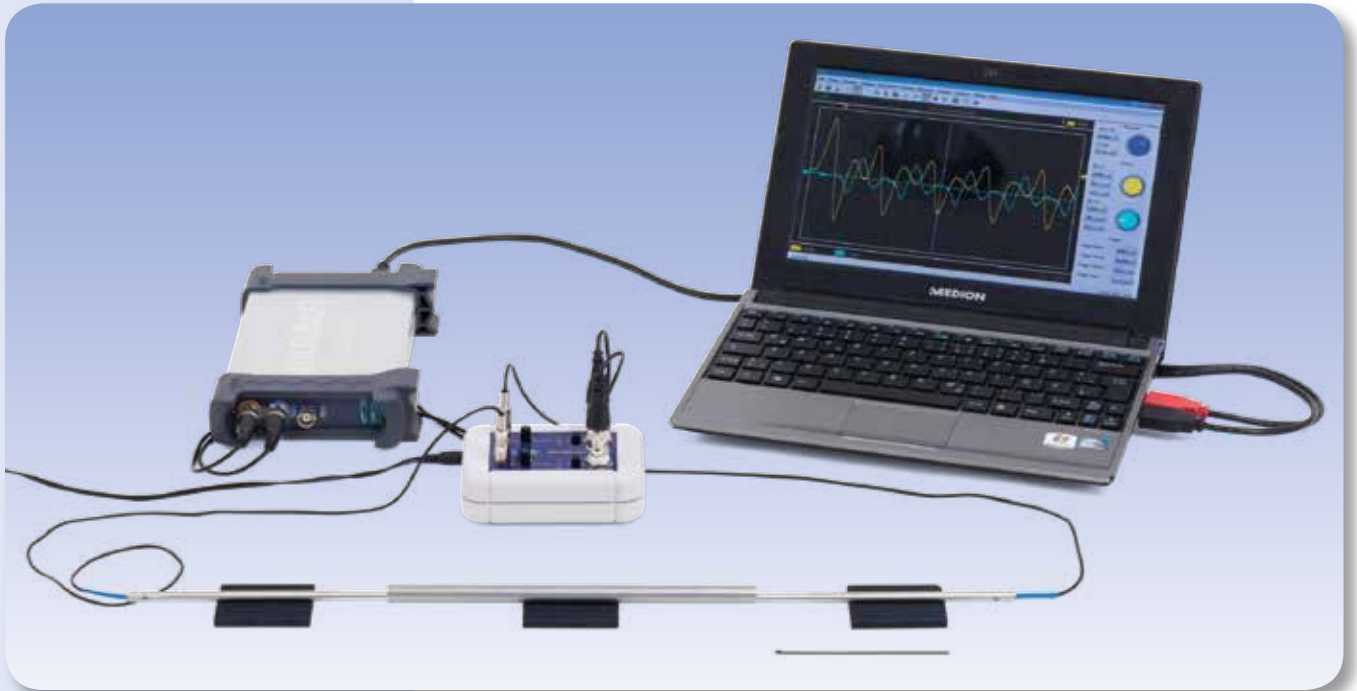


Fig. 2: Measured periods of oscillation T_1 and T_2 as a function of position of weight 2.



EXPERIMENT PROCEDURE

- Excite pulses of longitudinal sound waves in rods and use two microphone probes to detect them
- Analyse how the sound pulses are affected by the material and length of the rods by means of an oscilloscope
- Determine the speed of propagation of longitudinal sound waves in the materials from the time it takes the pulses to travel through them
- Determine the modulus of elasticity of the materials from the propagation velocity of longitudinal waves and their density



You can find technical information about the equipment at 3bscientific.com

2

OBJECTIVE

Investigation of longitudinal sound waves in cylindrical rods and determination of propagation velocity for longitudinal sound waves

SUMMARY

Sound waves can propagate through solids in the form of longitudinal, transverse, dilatational or flexural waves. An elastic longitudinal wave propagates along a rod by means of a periodic sequence of expansion and contraction along the length of the rod. The speed of propagation depends only on the modulus of elasticity and the density of the material when the diameter of the rod is small in comparison to its length. In this experiment, it will be determined from the time it takes sound pulses to travel along the rod.

REQUIRED APPARATUS

Quantity	Description	Number
1	Sound Propagation in Rods Equipment Set (230 V, 50/60 Hz)	1018469 or
	Sound Propagation in Rods Equipment Set (115 V, 50/60 Hz)	1018468
1	USB Oscilloscope 2x50 MHz	1017264
2	Patch Cord BNC, 0.5 m	5007670

BASIC PRINCIPLES

Sound waves can not only propagate in gases or liquids, but also in solid bodies. Longitudinal, transverse, dilatational or flexural waves can all occur in solids.

An elastic longitudinal wave propagates along a rod by means of a periodic sequence of expansion and contraction along the length of the rod. The expansion is caused by atoms being excited out of their rest positions. In a rod where the diameter is much smaller than the length, the contraction in the transverse direction is negligible, i.e. Poisson $\mu = 0$ to a good approximation. In this case, the

relationship between the changes in time and space of the compressive tension σ and the extension ξ is given by the following equations:

$$(1) \quad \frac{\partial \sigma}{\partial x} = \rho \cdot \frac{\partial v}{\partial t} \quad \text{and} \quad \frac{\partial v}{\partial x} = \frac{1}{E} \cdot \frac{\partial \sigma}{\partial t} \quad \text{where} \quad v = \frac{\partial \xi}{\partial t},$$

ρ : density of material of rod,

E : modulus of elasticity for material of rod

This results in the following wave equations:

$$(2) \quad \frac{\partial^2 \sigma}{\partial t^2} = \frac{E}{\rho} \cdot \frac{\partial^2 \sigma}{\partial x^2} \quad \text{and} \quad \frac{\partial^2 v}{\partial t^2} = \frac{E}{\rho} \cdot \frac{\partial^2 v}{\partial x^2}$$

The speed of propagation of longitudinal waves is

$$(3) \quad c_l = \sqrt{\frac{E}{\rho}}$$

In this experiment, longitudinal sound waves are excited in rods of various materials and lengths in the form of pulses. The pulses are then detected at the end of the rod being excited and at the other end by means of microphone sensors and displayed on an oscilloscope. The ends of the rod act as reflective surfaces for sound, such that the sound pulses reflect back and forth along the rods. The time it takes for pulses to travel from one end of the rod to the other is determined from the oscilloscope traces.

In long rods the multiply reflected sound pulses are clearly separated in time. In short rods, they could easily be superimposed and form “standing waves”.

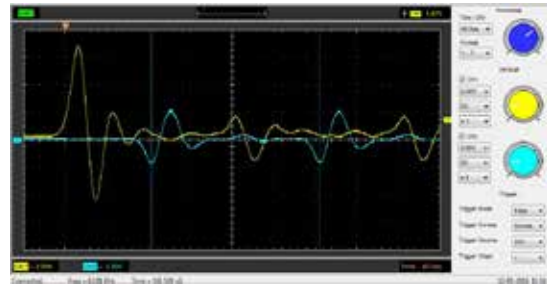


Fig. 1: Propagation of a sound pulse, signal at the excited end of the rod (yellow), (stainless steel rod, 400 mm)

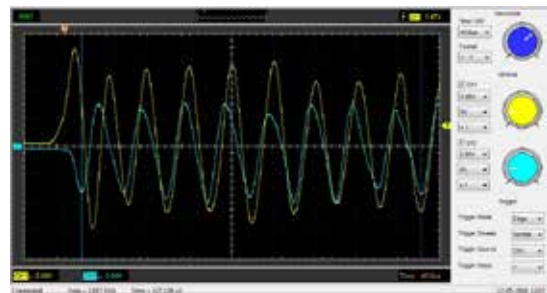


Fig. 2: Standing wave, signal at the excited end of the rod (yellow), (stainless steel rod, 100 mm)

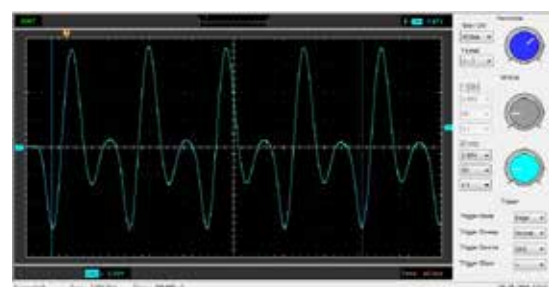
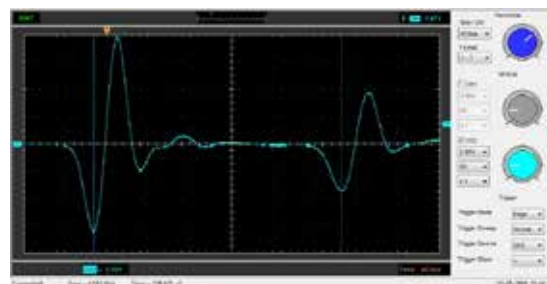


Fig. 3: Propagation of a sound pulse (top: PVC rod, 200 mm, bottom: glass rod, 200 mm), signal at the opposite end of the rod from the excitation (cyan)

EVALUATION

The velocity of the longitudinal sound waves is determined from the time they take to travel the length of the rod and back by means of the following equation:

$$(4) \quad c_l = \frac{2 \cdot L}{T}, \quad L: \text{Length of rod}$$

This is because the sound pulse travels the length of the rod twice (to the other end and back) in a time T .

The modulus of elasticity for each of the materials is determined using equation (3) from the speed of propagation measured and the density of the rods, as determined by weighing them.

Table 1: Speed of longitudinal sound waves c_l in various materials of density ρ and modulus of elasticity E .

Material	c_l (m / s)	ρ (g / cm ³)	E (m / s)
Glass	5370	2.53	73
Aluminium	5110	2.79	73
Wood (beech)	5040	0.74	19
Stainless steel	4930	7.82	190
Copper	3610	8.84	115
Brass	3550	8.42	106
Transparent acrylic (perspex)	2170	1.23	6
PVC	1680	1.50	4

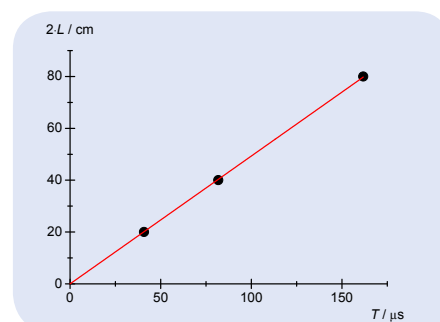
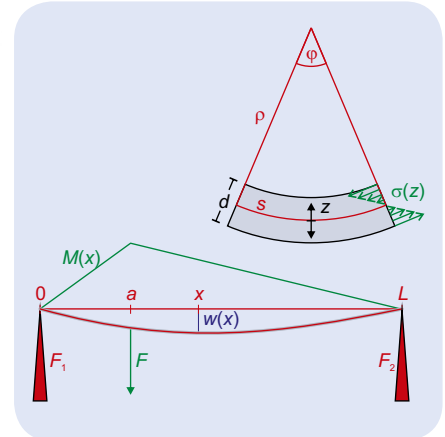
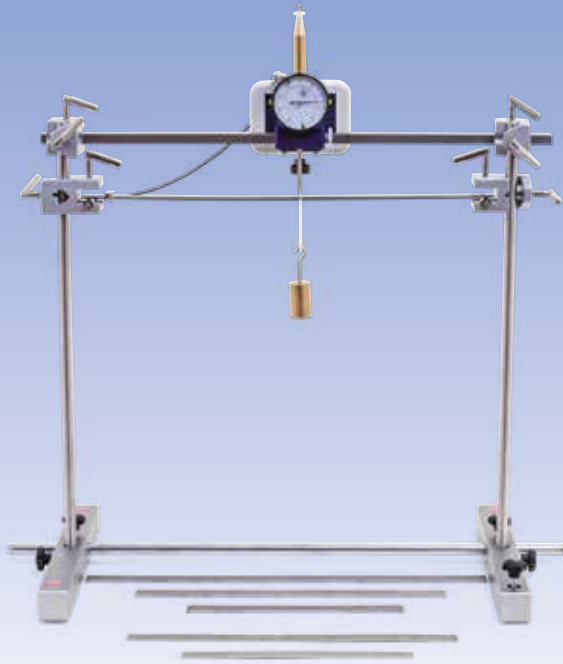


Fig. 4: Twice the length of the rods $2L$ as a function of the time of travel T for stainless steel rods.



OBJECTIVE

Measurement of deformation of flat beams supported at both ends and determination of modulus of elasticity

EXPERIMENT PROCEDURE

- Measure the deformation profile with loads in the centre and loads away from the centre.
- Measure the deformation as a function of the force.
- Measure the deformation as a function of the length, width and breadth as well as how it depends on the material and determine the modulus of elasticity of the materials.

SUMMARY

A flat, level beam's resistance to deformation in the form of bending by an external force can be calculated mathematically if the degree of deformation is much smaller than the length of the beam. The deformation is proportional to the modulus of elasticity E of the material from which the beam is made. In this experiment, the deformation due to a known force is measured and the results are used to determine the modulus of elasticity for both steel and aluminium.

REQUIRED APPARATUS

Quantity	Description	Number
1	Apparatus for Measuring Young's Modulus	1018527
1	Young's Modulus Supplementary Set	1018528
1	Pocket Measuring Tape, 2 m	1002603
1	External Micrometer	1002600

BASIC PRINCIPLES

A flat, level beam's resistance to deformation in the form of bending by an external force can be calculated mathematically if the degree of deformation is much smaller than the length of the beam. The deformation is proportional to the modulus of elasticity E of the material from which the beam is made. Therefore the deformation due to a known force can be measured and the results are used to determine the modulus of elasticity.

For the calculation, the beam is sliced into parallel segments which are compressed on the inside by the bending and stretched on the outside. Neutral segments undergo no compression or extension. The relative extension or compression ϵ of the other threads and the associated tension σ depends on their distance z from the neutral segments:

$$(1) \quad \epsilon(z) = \frac{s + \Delta s(z)}{s} = \frac{z}{\rho(x)} \quad \text{and} \quad \sigma(z) = E \cdot \epsilon(z)$$

$\rho(x)$: Local radius of curvature due to bending



You can find technical information about the equipment at 3bscientific.com

2

The curvature therefore involves the local bending moment:

$$(2) \quad M(x) = \int_A \sigma(z) \cdot z \cdot dA = \frac{1}{\rho(x)} \cdot E \cdot I$$

where $I = \int_A z^2 \cdot dA$: Area moment of inertia

As an alternative to the radius of curvature $\rho(x)$, in this experiment the deformation profile $w(x)$, by which the neutral segments are shifted from their rest position, will be measured. This can be calculated as follows, as long as the changes $dw(x)/dx$ due to the deformation are sufficiently small:

$$(3) \quad \frac{d^2 w}{dx^2}(x) = \frac{1}{\rho(x)} = \frac{M(x)}{E \cdot I},$$

the deformation profile is obtained from this by double integration.

A typical example is to observe a beam of length L , which is supported at both ends and to which a downward force F acts at a point a . In a state of equilibrium the sum of all the forces acting is zero:

$$(4) \quad F_1 + F_2 - F = 0$$

Similarly, the sum of all the moments acting on the beam at an arbitrary point x is also zero:

$$(5) \quad M(x) - F_1 \cdot x - F_2 \cdot (L - x) + F \cdot (a - x) = 0$$

No curvature or deformation arises at the ends of the beam, i.e. $M(0) = M(L) = 0$ and $w(0) = w(L) = 0$. This means that $M(x)$ is fully determinable:

$$(6) \quad M(\zeta) = \begin{cases} F \cdot L \cdot (1 - \alpha) \cdot \zeta; & 0 \leq \zeta \leq \alpha \\ F \cdot L \cdot \alpha \cdot (1 - \zeta); & \alpha < \zeta \leq 1 \end{cases}$$

where $\zeta = \frac{x}{L}$ and $\alpha = \frac{a}{L}$

The deformation profile is obtained by double integration

$$(7) \quad w(\zeta) = \begin{cases} \frac{F \cdot L^3}{E \cdot I} \cdot \left[(1 - \alpha) \cdot \frac{\zeta^3}{6} - \left(\frac{\alpha^3}{6} - \frac{\alpha^2}{2} + \frac{\alpha}{3} \right) \cdot \zeta \right] \\ \frac{F \cdot L^3}{E \cdot I} \cdot \left[\frac{\alpha^3}{6} - \left(\frac{\alpha^3}{6} + \frac{\alpha}{3} \right) \zeta + \frac{\alpha}{2} \cdot \zeta^2 - \frac{\alpha}{6} \zeta^3 \right] \end{cases}$$

In the experiment the shape of this profile is checked for load at the centre ($\alpha = 0.5$) and off-centre ($\alpha < 0.5$).

EVALUATION

When the load is in the centre, then $w(x = \frac{L}{2}, a = \frac{L}{2}) = -\frac{F \cdot L^3}{48 \cdot E \cdot I}$

For a rectangle of width b and height d , the following calculation is made:

$$I = \int_A z^2 \cdot dA = \int_{-\frac{d}{2}}^{\frac{d}{2}} z^2 \cdot b \cdot dz = \frac{d^3}{12} \cdot b$$

Then $w(x = \frac{L}{2}, a = \frac{L}{2}) = -\frac{1}{4} \cdot \frac{F}{E} \cdot \frac{L^3}{d^3} \cdot \frac{1}{b}$

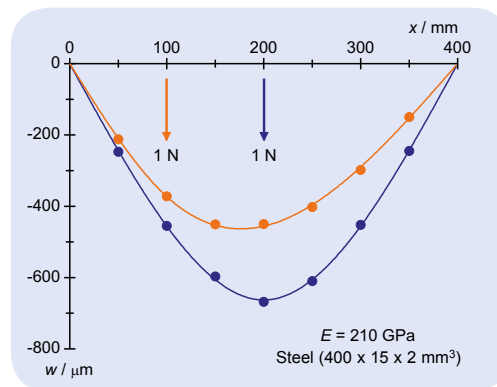


Fig. 1: Measured and calculated deformation profile for load acting at centre and off-centre

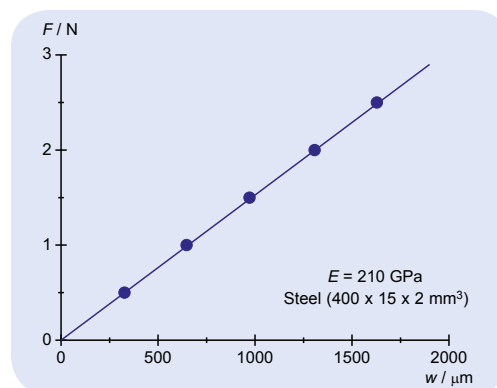


Fig. 2: Confirmation of Hooke's law

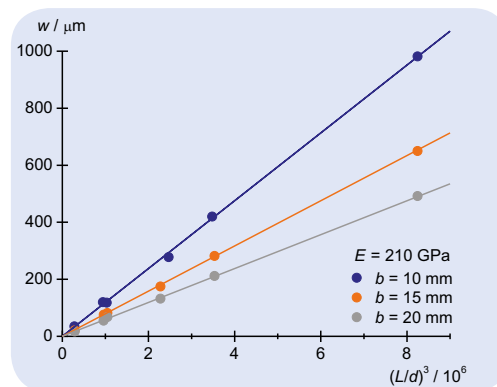


Fig. 3: How the deformation depends on $(L/d)^3$

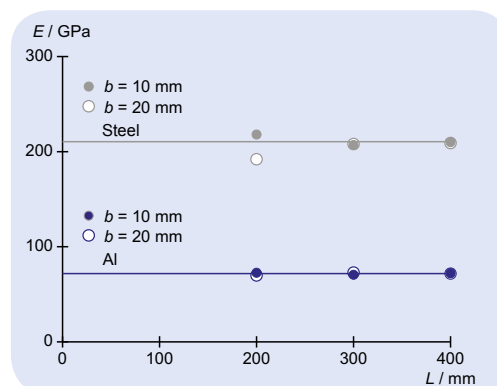
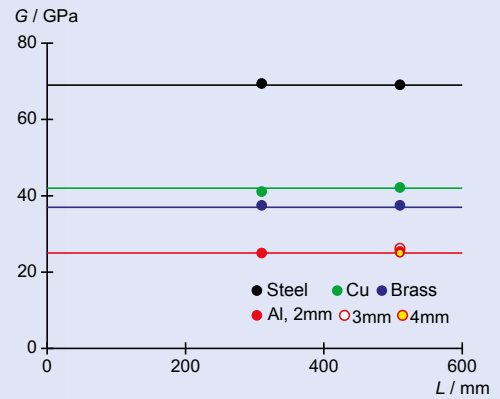


Fig. 4: Modulus of elasticity of steel and aluminium

UE1090300

TORSION ON CYLINDRICAL RODS



OBJECTIVE

Determination of torsional coefficients and shear modulus

EXPERIMENT PROCEDURE

- Determine the torsional coefficients of cylindrical rods as a function of their length.
- Determine the torsional coefficients of cylindrical rods as a function of their diameter.
- Determine the torsional coefficients of cylindrical rods made of various materials and also find their shear modulus.



You can find technical information about the equipment at 3bscientific.com

2

SUMMARY

In order for solid bodies to be deformed, an external force needs to be applied. This acts against the body's own resistance to deformation, which is dependent on the material from which the body is made, as well as its geometry and the direction of the applied force. The deformation is reversible and proportional to the applied force as long as that force is not too great. One example which is often investigated is torsion applied to a uniform cylindrical rod which is fixed at one end. The resistance of the rod to deformation can be numerically analysed and determined by building a set-up which is capable of oscillating involving the rod itself and a pendulum disc and then measuring the period of the oscillation.

REQUIRED APPARATUS

Quantity	Description	Number
1	Torsion Apparatus	1018550
1	Supplementary Set for Torsion Apparatus	1018787
1	Photo Gate	1000563
1	Digital Counter (230 V, 50/60 Hz)	1001033 or
	Digital Counter (115 V, 50/60 Hz)	1001032

BASIC PRINCIPLES

In order for solid bodies to be deformed, an external force needs to be applied. This acts against the body's own resistance to deformation, which is dependent on the material from which the body is made, as well as its geometry and the direction of the applied force. The deformation is elastic, reversible and proportional to the applied force as long as that force is not too great.

One example which is often investigated is torsion applied to a uniform cylindrical rod which is fixed at one end because the resistance of the rod to deformation can be numerically analysed. This involves

considering the rod broken down into radial and cylindrical segments of length L . As long as the rod does not bend, then the torsion applied to the rod at the non-fixed end which twists that end of the rod by a small angle ψ causes each of the segments, which are all of radius r , to twist by the following angle:

$$(1) \quad \alpha_r = \frac{r}{L} \cdot \psi$$

(see Fig. 1). The shearing stress would then be:

$$(2) \quad \tau_r = \frac{dF_{r,\varphi}}{dA_{r,\varphi}} = G \cdot \alpha_r$$

G : Shear modulus of the rod's material

The component of the force $dF_{r,\varphi}$ acting in tangential direction at the face of the rod:

$$(3) \quad \Delta A_{r,\varphi} = r \cdot d\varphi \cdot dr$$

is given by:

$$(4) \quad dF_{r,\varphi} = G \cdot \frac{r^2}{L} \cdot \psi \cdot d\varphi \cdot dr.$$

It is then easy to calculate the force dF_r required for the torsion to twist the whole of a hollow cylinder of radius r by an angle ψ along with the corresponding torque dM_r :

$$(5) \quad dM_r = r \cdot dF_r = G \cdot 2\pi \cdot \frac{r^3}{L} \cdot \psi \cdot dr$$

Then for a solid rod of radius r_0 , the torsion can be found as follows:

$$(6) \quad M = \int_0^{r_0} dM_r = D \cdot \psi \quad \text{where} \quad D = G \cdot \frac{\pi}{2} \cdot \frac{r_0^4}{L}$$

The torque M remains proportional to the angle of twist resulting from the torsion ψ , i.e. the torsional coefficient D is constant, as long as the torque M is not too large. If the torque is too high, then the deformation becomes plastic and irreversible.

In order to determine the torsional coefficient in this experiment, a pendulum disc is coupled to the non-fixed end of the rod. As long as the angle of deflection is not too great, the disc will oscillate about the torsional axis with a period

$$(7) \quad T = 2\pi \cdot \sqrt{\frac{J}{D}},$$

J : Moment of inertia of pendulum disc

As long as the moment of inertia is known, the torsional coefficient can be determined from the period of oscillation. To be more precise, the overall moment of inertia is split into the moment of inertia J_0 for the pendulum disc and the moment of inertia of the two additional weights m , which are situated at a radius R around the torsional axis:

$$(8) \quad J = J_0 + 2 \cdot m \cdot R^2$$

The period of oscillation T for the pendulum disc with the additional weights is then measured along with the period of oscillation T_0 for the pendulum disc without the weights.

EVALUATION

The equation for determining the torsional coefficient is derived from equations (7) and (8) as follows:

$$D = 4\pi^2 \cdot \frac{2 \cdot m \cdot R^2}{T^2 - T_0^2}$$

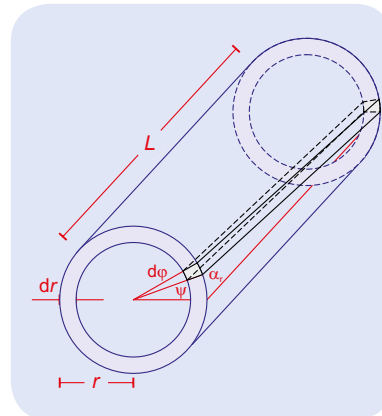


Fig. 1: Schematic for the calculation of the torque dM_r needed to apply torsion on a hollow cylinder of length L , radius r and shell thickness d_r .

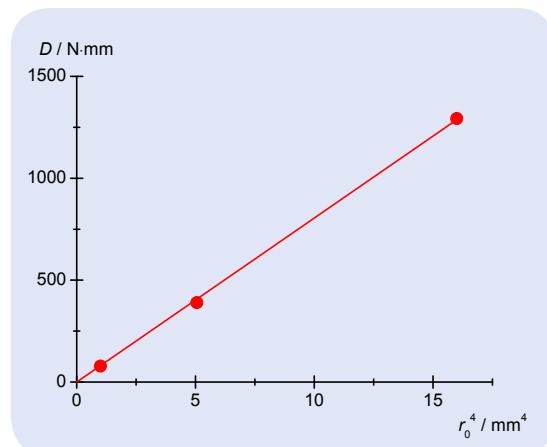


Fig. 2: Torsional coefficient of aluminium rods 500 mm in length as a function of r_0^4 .

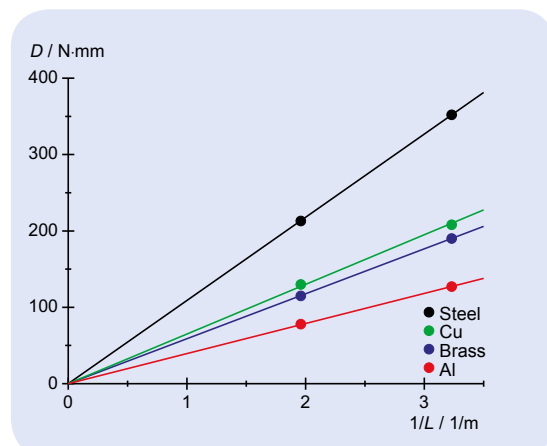


Fig. 3: Torsional coefficient of cylindrical rods as a function of $1/L$.

UE2040120

AMONTONS' LAW**EXPERIMENT PROCEDURE**

- Point-by-point measurement of the pressure p of the enclosed air as a function of the temperature T .
- Plotting the measured values in a p - T diagram.
- Verification of Amontons' law.



You can find technical information about the equipment at 3bscientific.com

1**OBJECTIVE**

Verify the linear relationship between the pressure and temperature of an ideal gas

SUMMARY

The validity of Amontons' law for ideal gases is demonstrated using normal air. To demonstrate this, a volume of enclosed air located in a hollow metallic sphere is heated with the aid of a water bath while the temperature and pressure are being measured at the same time.

REQUIRED APPARATUS

Quantity	Description	Number
1	Jolly's Bulb and Gauge	1012870
1	Magnetic Stirrer with Heater (230 V, 50/60 Hz)	1002807 or
	Magnetic Stirrer with Heater (115 V, 50/60 Hz)	1002806
1	Digital Quick Response Pocket Thermometer	1002803
1	K-Type NiCr-Ni Immersion Sensor, -65°C – 550°C	1002804
1	Set of 10 Beakers, Low Form	1002872
1	Tripod Stand 150 mm	1002835
1	Stainless Steel Rod 250 mm	1002933
1	Bosshead	1002827
1	Universal Jaw Clamp	1002833

BASIC PRINCIPLES

The volume of a quantity of gas depends on the pressure the gas is under and on its temperature. When the volume and the gas quantity remain constant, the quotient comprising the pressure and the temperature remains constant. The law discovered by *Guillaume Amontons* applies for gases in the ideal state, i.e. when the temperature of the gas is far in excess of its so-called critical temperature.

The law discovered by Amontons

$$(1) \quad \frac{p}{T} = \text{const.}$$

is a special case of the universal gas law valid for all ideal gases, which describes the relationship between the pressure p , the volume V , temperature T relative to absolute zero and the mass n of a gas:

$$(2) \quad p \cdot V = n \cdot R \cdot T$$

$$R = 8,314 \frac{\text{J}}{\text{mol} \cdot \text{K}}: \text{universal gas constant}$$

Based on the generally applicable Equation (2) the special case (1) can be derived under the precondition that the volume V and the mass of the enclosed gas n do not change.

In the experiment the validity of Amontons' law is demonstrated using air as the ideal gas. To do this the enclosed volume of air located in a hollow metal sphere is heated up with the aid of a water bath. At the same time the temperature ϑ is measured in °C using a digital thermometer and the pressure p is measured using a manometer attached to the hollow sphere.

EVALUATION

The linear relationship between pressure and temperature is confirmed by fitting a straight line

$$(3) \quad p = a \cdot \vartheta + b$$

to the measurement points. By extrapolating the pressure p up to a value of 0, the absolute zero temperature can be determined:

$$(4) \quad \vartheta_0 = -\frac{b}{a} [\text{°C}]$$

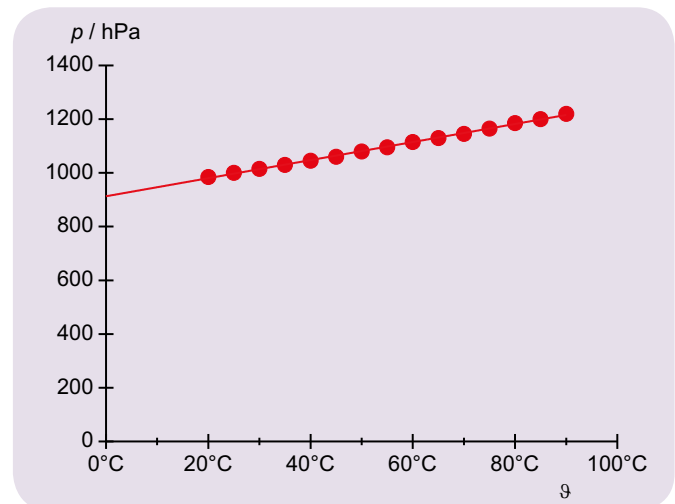


Fig. 1: Pressure-temperature diagram of air at constant volume and constant mass.

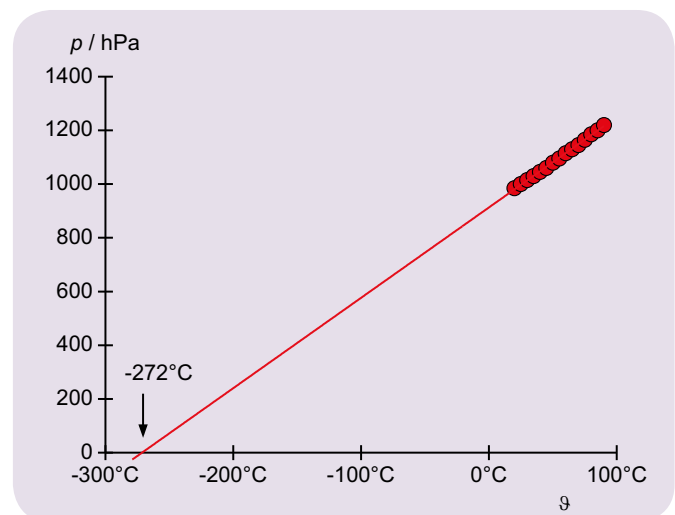


Fig. 2: Extrapolation of the pressure to a value of $p = 0$.

UE3030350

ELECTRIC BALANCE**EXPERIMENT PROCEDURE**

- Measurement of the force exerted on a current-carrying conductor as a function of the amperage.
- Measurement of the force exerted on a current-carrying conductor as a function of its length.
- Calibration of the magnetic field.



You can find technical information about the equipment at 3bscientific.com

1**OBJECTIVE**

Measurement of the force exerted on a current-carrying conductor located inside a magnetic field

SUMMARY

The electric balance is based on *André-Marie Ampères'* experiments on electric current. It measures the electro-dynamic force sometimes referred to as the Lorentz force on a current carrying conductor situated in a magnetic field using a balance. In this experiment the current conductor is suspended from a rigid suspension system and exerts the equal and opposite force on the permanent magnets as the electro-dynamic force generated by the magnetic field. The result is the apparent change in weight of the permanent magnets.

REQUIRED APPARATUS

Quantity	Description	Number
1	Current Balance Equipment Set	1019188
1	Electronic Scale Scout Pro 200 g (230 V, 50/60 Hz)	1009772
1	DC Power Supply 0 – 20 V, 0 – 5 A (230 V, 50/60 Hz)	1003312
1	Stainless Steel Rod 250 mm	1002933
1	Tripod Stand 150 mm	1002835
1	Two-pole Switch	1018439
3	Pair of Experiment Leads, 75 cm	1002850

BASIC PRINCIPLES

The electric balance is based on *André-Marie Ampères'* experiments on electrical current. It measures the force exerted on a current-carrying conductor located in a magnetic field with the aid of a balance. In the experiment a modern electronic precision balance weighs a permanent magnet. The weight measured changes in accordance with Newton's 3rd law when an electro-dynamic force is exerted on a current-carrying conductor entering a magnetic field.

On the balance lies a permanent magnet which generates a horizontal magnetic field B . In this arrangement a horizontal current conductor of length L and suspended from a rigid bar is dipped vertically into the magnetic field. The electro-dynamic force from the magnet acts on the conductor

$$(1) \quad F_L = N \cdot e \cdot v \times B,$$

e : elementary charge,
 N : total number of all electrons participating in electrical conduction

The mean drift velocity v is all the greater, the greater the current I flowing through the conductor:

$$(2) \quad I = n \cdot e \cdot A \cdot v$$

n : number of all electrons involved in the current conduction,
 A : cross-section of the conductor

From

$$(3) \quad N = n \cdot A \cdot L$$

L : length of the conductor

we obtain

$$(4) \quad F_L = I \cdot L \cdot e \times B$$

or

$$(5) \quad F_L = I \cdot L \cdot B$$

since the unit vector e pointing in the direction of the conductor is located perpendicular to the magnetic field. In accordance with Newton's third law, an equal and opposite force F is exerted on the permanent magnet. Depending on the sign, the weight G of the permanent magnet measured on the balance is either increased or decreased. Thanks to the balance's tare function, the weight G can be electronically offset so that the balance immediately displays the opposing force F .

EVALUATION

It has been demonstrated that the current dependency of the electro-dynamic force or Lorentz force can be accurately described by a straight line through the origin (Fig. 2). This is not the case for conductor length dependency (Fig. 3) due to the fact that here boundary effects play a role at the ends of the conductor. The magnetic field of the fully assembled permanent magnet is computed from the linear gradients $a_2 = B L$ in Fig. 2 and $a_3 = B I$ in Fig. 3.

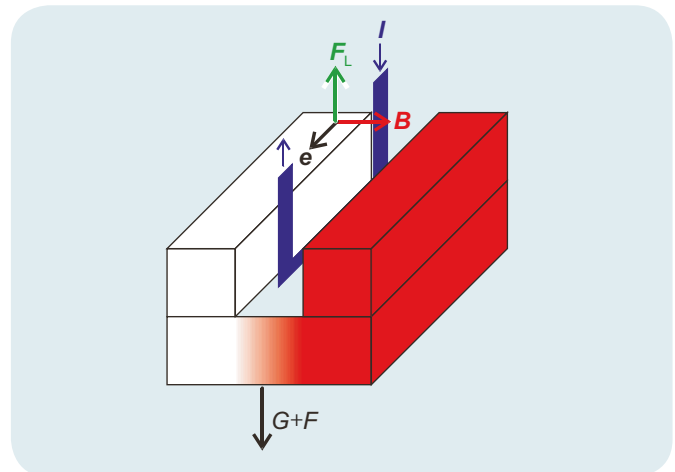


Fig. 1: Schematic depiction of the electro-dynamic force F_L on the current-carrying conductor and the total force $G + F$ on the balance.

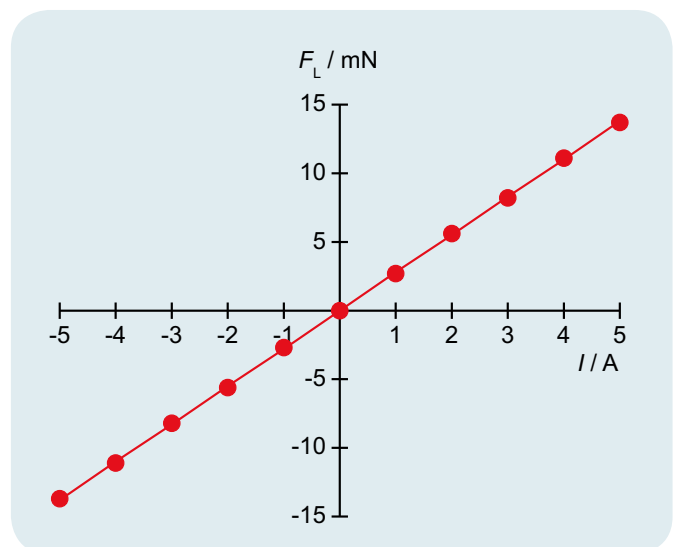


Fig. 2: Force F_L as a function of the amperage I

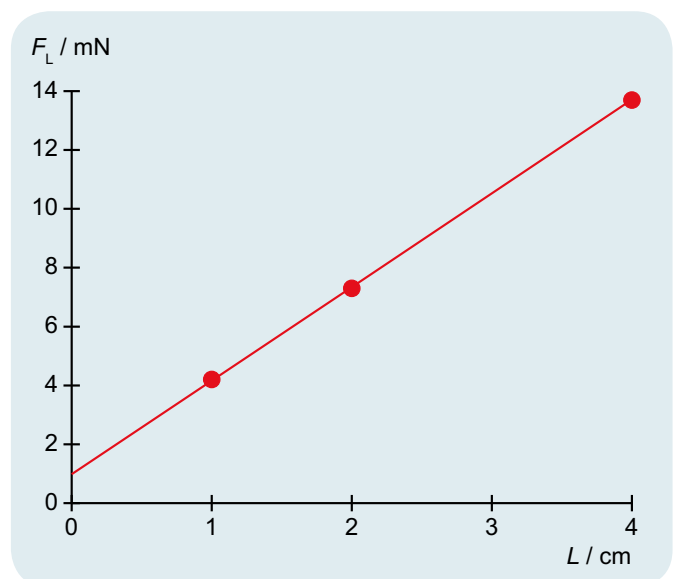
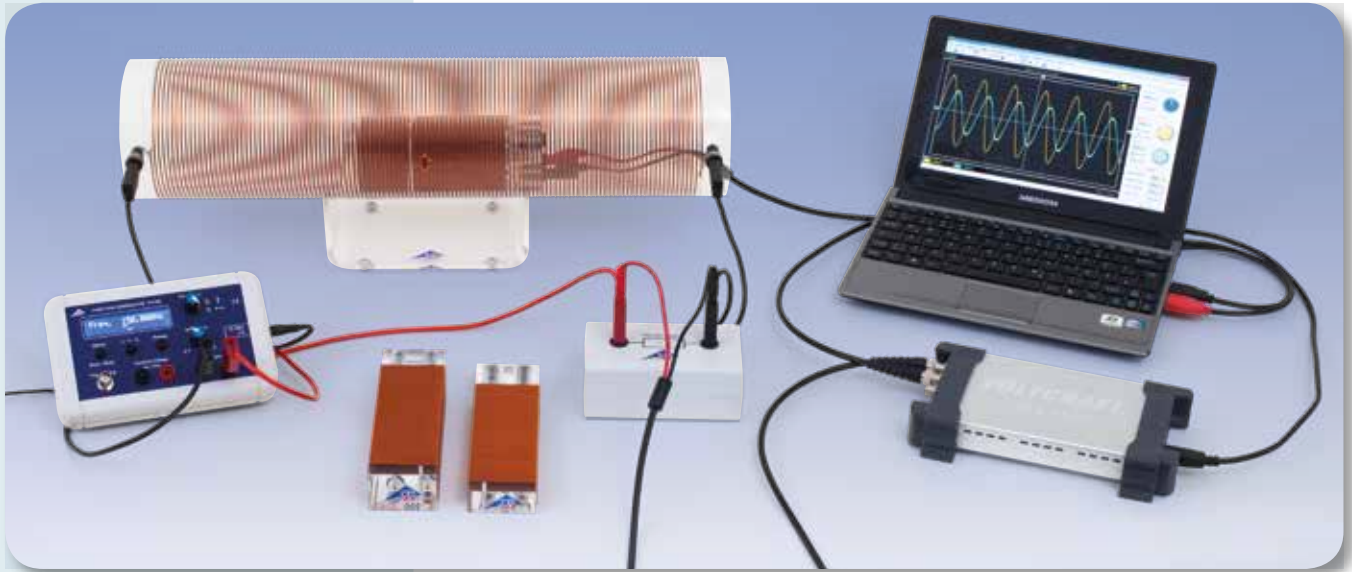


Fig. 3: Force F_L as a function of the conductor length L

UE3040300

**INDUCTION THROUGH A VARYING
MAGNETIC FIELD****EXPERIMENT
PROCEDURE**

- Measure the induced voltage as a function of the number of turns N of the induction coil.
- Measure the induced voltage as a function of the cross-sectional area A of the induction coil.
- Measure the induced voltage as a function of the amplitude I_0 of the alternating current applied for induction.
- Measure the induced voltage as a function of the frequency f of the alternating current applied for induction.
- Measure the induced voltage as a function of the waveform of the alternating current applied for induction.



You can find technical information about the equipment at 3bscientific.com

1**OBJECTIVE**

Measuring the voltage induced in an induction coil

SUMMARY

If a closed conductor loop with N windings is located in a cylinder coil through which an alternating current flows, then an electrical voltage is induced by the variable magnetic flux through the conductor loop. This induction voltage is dependent on the number of windings and the cross-sectional area of the conductor loop as well as the frequency, amplitude and waveform of alternating current applied to the field coil. These dependencies are explored and compared with the principle theory.

REQUIRED APPARATUS

Quantity	Description	Number
1	Set of 3 Induction Coils	1000590
1	Field Coil 120 mm	1000592
1	Stand for Cylindrical Coils	1000964
1	Precision Resistor 1 Ω	1009843
1	Function Generator FG 100 (230 V, 50/60 Hz)	1009957 or
	Function Generator FG 100 (115 V, 50/60 Hz)	1009956
1	USB Oscilloscope 2x50 MHz	1017264
2	HF Patch Cord, BNC/4 mm Plug	1002748
1	Pair of Safety Experiment Leads, 75 cm, black	1002849
1	Pair of Safety Experimental Leads, 75 cm, red/blue	1017718

BASIC PRINCIPLES

Every change in the magnetic flux through a closed conductor loop with N turns induces an electrical voltage in said loop. Such a variation is evoked, for example, if the conductor loop is located in a cylinder coil which has alternating current flowing through it.

According to Faraday's law of induction the following applies for an induced voltage dependent on rate of change:

$$(1) \quad U(t) = -N \cdot \frac{d\Phi}{dt}(t).$$

The magnetic flux Φ through an area A is given by:

$$(2) \quad \Phi = B \cdot A$$

B : Magnetic flux density

if the magnetic flux density B permeates the area A perpendicularly. Consequently, from Equation (1) we obtain:

$$(3) \quad U(t) = -N \cdot A \cdot \frac{dB}{dt}(t).$$

The field coil generates the following magnetic flux density in the conductor loop:

$$(4) \quad B = \mu_0 \cdot \frac{N_F}{L_F} \cdot I$$

$\mu_0 = 4\pi \cdot 10^{-7} \text{ N/A}^2$: Vacuum permeability, N_F : Number of turns in the field coil, L_F : Length of the field coil, I : Current flowing through the field coil

Accordingly, from Equation (3) we arrive at:

$$(5) \quad U(t) = -\mu_0 \cdot N \cdot A \cdot \frac{N_F}{L_F} \cdot \frac{dI}{dt}(t).$$

In the experiment a function generator is used first to apply a sinusoidal signal to the field coil. The amplitude I_0 of the current $I(t)$ is determined by the field coil with the aid of a resistor connected in series between the coil and generator. The amplitude U_0 of the induced voltage $U(t)$ is measured as a function of the number of windings N and cross-sectional area A of the induction coils as well as the frequency f of the sinusoidal signal and the amplitude I_0 of the current flowing through the field coil.

Besides the sinusoidal signal, a triangular and a square-wave signal are also applied to the field coil for an induced voltage on a coil with fixed number of turns and cross-sectional area as well as a constant frequency, and from these measurements screen shots are made for each.

EVALUATION

For sinusoidal current:

$$I = I(t) = I_0 \cdot \sin(2 \cdot \pi \cdot f \cdot t),$$

the following applies:

$$U(t) = U_0 \cdot [-\cos(2 \cdot \pi \cdot f \cdot t)]$$

with:

$$U_0 = 2 \cdot \pi \cdot \mu_0 \cdot \frac{N_F}{L_F} \cdot N \cdot A \cdot I_0 \cdot f.$$

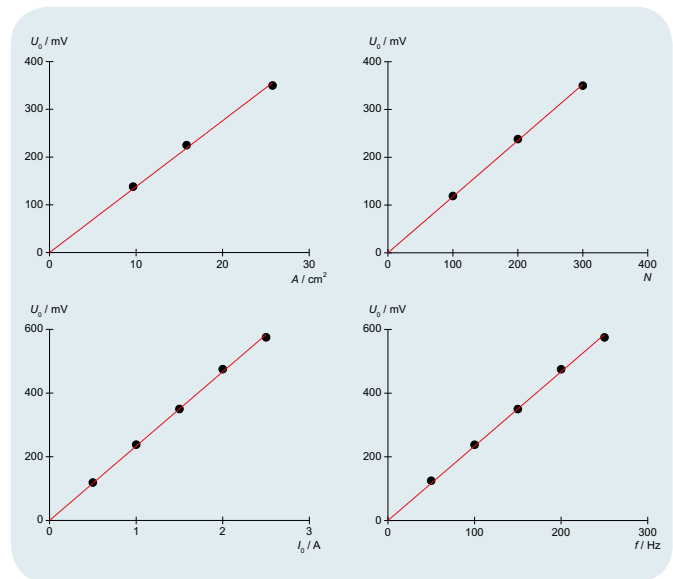


Fig. 1: Amplitude of the induced voltage as a function of the number of turns and the cross-sectional area of the induction coil as well as the amplitude of the current flowing through the field coil and the frequency of the sinusoidal signal applied to the field coil.

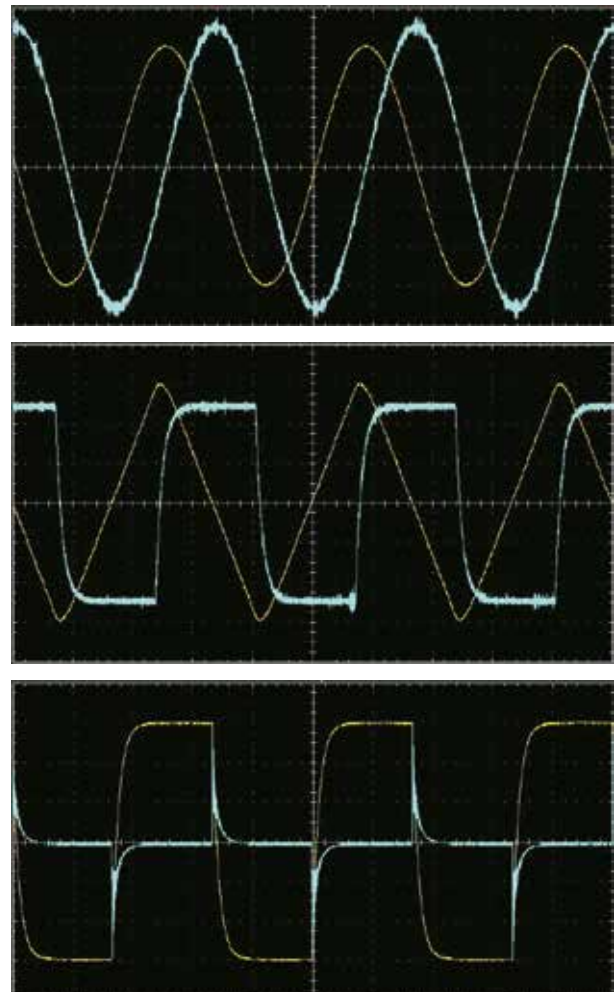


Fig. 2: Screen shots of the characteristics of the induced voltage as a function of time for a sinusoidal (top left), triangular (top right) and square-wave signal (bottom) applied to the field coil

UE4010000

REFLECTION IN A MIRROR



EXPERIMENT PROCEDURE

- Demonstrate the law of reflection using a plane mirror.
- Determine the focal length of a concave mirror and demonstrate that it too obeys the law of reflection.
- Determine the virtual focal length of a convex mirror.

OBJECTIVE

Investigate reflection from a plane mirror and a curved mirror

SUMMARY

Light rays are reflected by a mirror such that the angle of incidence is equal to the angle of reflection. This law of reflection applies not only to plane mirrors but also to curved ones. Only plane mirrors, though, reflect parallel incident rays in such a way that they remain parallel upon reflection. This is because the angle of incidence of all these parallel rays will be the same. For curved mirrors, concave and convex, parallel rays do not remain parallel after reflection. Instead, they are focussed towards a focal point.

REQUIRED APPARATUS

Quantity	Description	Number
1	Optical Bench U, 1200 mm	1003039
3	Optical Rider U, 75 mm	1003041
1	Optical Rider U, 35 mm	1003042
1	Optical Lamp with LED	1020630
1	Iris on Stem	1003017
1	Object Holder on Stem	1000855
1	Optical Disc with Accessories	1003036
1	Set of 5 Slit and Hole Diaphragms	1000607

BASIC PRINCIPLES

Light rays are reflected by a mirror such that the angle of incidence is equal to the angle of reflection. This law of reflection applies not only to plane mirrors but also to curved ones. Only plane mirrors, though, reflect parallel incident rays in such a way that they remain parallel upon reflection. This is because the angle of incidence of all these parallel rays will be the same.

If parallel light rays strike a plane mirror at angle α , the law of reflection indicates that they should be reflected to an angle β :

$$(1) \quad \alpha = \beta$$

α : Angle of incidence, β : Angle of reflection

In this experiment the angle of reflection will be measured directly for three parallel beams and it will be determined how this angle is related to the angle of incidence.

If a light ray which is parallel to the optical axis is incident upon a concave mirror, the law of reflection says that it will be reflected symmetrically about a normal to the point of incidence and will then cross the optical axis at the following distance from the mirror:



You can find technical information about the equipment at 3bscientific.com

1

$$(2) \quad f_{\alpha} = r - \overline{MF} = r \cdot \left(1 - \frac{1}{2 \cdot \cos \alpha}\right).$$

(See Fig. 1 for path of rays on left-hand side). For rays close to the optical axis itself, $\cos \alpha$ is close to 1, therefore

$$(3) \quad f = \frac{r}{2}.$$

This is not dependent on the distance from the optical axis, which means that all parallel rays near to the optical axis will, after reflection, converge at the same point (the focal point) on the optical axis a distance f (the focal length) from the surface of the concave mirror. If parallel rays strike the mirror at an angle α to the optical axis, they will be reflected through a common point away from the optical axis. The geometric relationships for a convex mirror are similar to those for a concave mirror except that the rays diverge rather than converge after reflection. The diverging rays, however, do appear to have a point of convergence at a virtual focal point f' behind the mirror (see Fig. 1 for path of rays on right-hand side). The virtual focal length f' for a convex mirror is given by the following:

$$(4) \quad f' = -\frac{r}{2}.$$

In the experiment the focal length of the concave mirror and the virtual focal length of the convex mirror will be determined from the paths of the rays on an optical disc. The validity of the law of reflection will be checked for the ray in the centre.

EVALUATION

Parallel light rays incident upon a plane mirror are reflected back as parallel rays. The law of reflection applies to this process.

When a beam of parallel rays is reflected by a concave mirror, the angle of incidence is different for each of the rays and all the rays are then focussed towards a focal point.

Similarly, when a beam of parallel rays is reflected by a convex mirror, the rays converge at a virtual focal point behind the mirror.

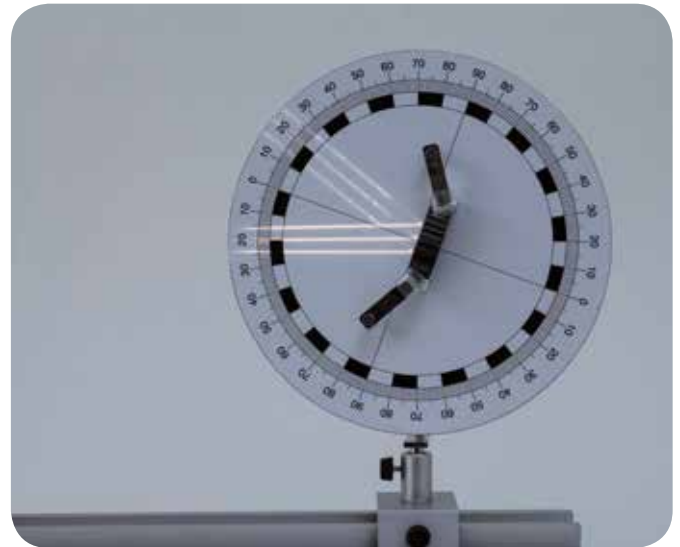


Fig. 2: Reflection of three parallel rays by a plane mirror



Fig. 3: Reflection of three parallel rays by a concave mirror

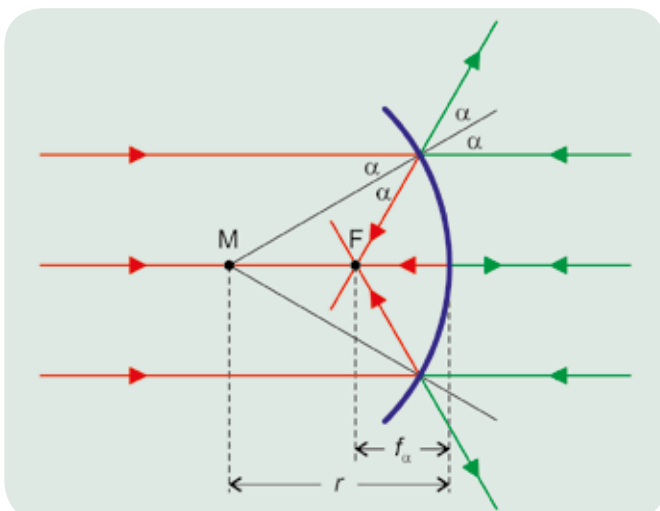


Fig. 1: Schematic for determining focal length of a concave mirror and a convex mirror

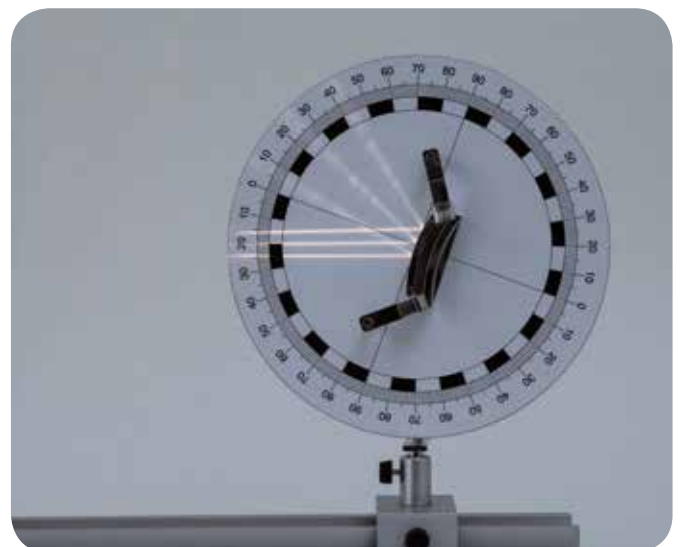


Fig. 4: Reflection of three parallel rays by a convex mirror



EXPERIMENT PROCEDURE

- Verify Snell's law of refraction.
- Determine the refractive index and the critical angle for total internal reflection for transparent acrylic plastic.
- Observe and measure how a beam deviates along a different parallel path when refracted by a rectangular block.
- Observe the path of light inside a prism which merely deflects a beam and in one which reverses it.
- Observe the path of light inside a convex lens and in a concave lens and determine their focal lengths.



You can find technical information about the equipment at 3bscientific.com

1

OBJECTIVE

Investigate refraction of light by various optical components

SUMMARY

Light propagates at different speeds in different media. If a medium has low optical depth, the speed of propagation is higher than it would be in a medium of greater optical depth. A change in direction therefore takes place when a beam of light passes through a boundary between two media at any non-zero angle of incidence. The degree of deflection is dependent on the ratio of the refractive indices of these two media, as described by Snell's law of refraction. This refractive behaviour will now be investigated using optical components made of transparent acrylic (perspex).

REQUIRED APPARATUS

Quantity	Description	Number
1	Optical Bench U, 1200 mm	1003039
3	Optical Rider U, 75 mm	1003041
1	Optical Rider U, 35 mm	1003042
1	Optical Lamp with LED	1020630
1	Iris on Stem	1003017
1	Object Holder on Stem	1000855
1	Optical Disc with Accessories	1003036
1	Set of 5 Slit and Hole Diaphragms	1000607

BASIC PRINCIPLES

Light propagates at different speeds c in different media. If a medium has low optical depth, the speed of propagation is higher than it would be in a medium of greater optical depth.

The ratio of the speed of light in a vacuum c_0 to the speed within the medium is called the absolute refractive index n . If the speed of light in the medium is c , then the following is true:

$$(1) \quad c = \frac{c_0}{n}$$

When a beam of light passes from one medium of refractive index n_1 to another one of refractive index n_2 , the beam changes direction at the boundary. This is described by Snell's law of refraction:

$$(2) \quad \frac{\sin \alpha}{\sin \beta} = \frac{n_1}{n_2} = \frac{c_2}{c_1}$$

α, n_1, c_1 : angle of incidence, refractive index and speed of propagation in medium 1

β, n_2, c_2 : angle of refraction, refractive index and speed of propagation in medium 2

A beam of light passing from a medium of relatively low optical depth into one of higher optical depth will be refracted towards a normal to the boundary surface and a beam passing from a medium of higher optical depth into one of lower optical depth would be refracted away from the normal. In the latter case, there is also a critical angle α_c , at which the beam is actually refracted along the boundary surface. At greater angles of incidence than this, refraction does not take place at all and the beam is totally reflected.

This refractive behaviour is investigated in this experiment using a semi-circular body, a rectangular block with parallel sides, a prism, a converging lens and a dispersing lens, all made of transparent acrylic. The semi-circular body is particularly well suited to demonstrating the law of refraction since no refraction takes place at the semi-circular perimeter if the beam strikes the flat surface precisely at the centre of the circle. The flat side forms the boundary between media and will be aligned at various angles to the optical axis (see Fig. 1).

As a beam of light is refracted on entering and on exiting a rectangular block, it is deflected along a line parallel to its original direction but a distance d away from that line. The deflected distance is dependent on the angle of incidence α . The following applies (see Fig. 1):

$$(3) \quad d = h \cdot \frac{\sin(\alpha - \beta)}{\cos \beta}, \quad h: \text{thickness of block.}$$

A 90° prism will act in such a way as to deflect a beam of light if light beams strike it perpendicular to one of the short sides. The beam is then reflected at the hypotenuse and exits the prism having been deflected by 90°. If, however the beam strikes perpendicular to the hypotenuse, it is reflected by both the other sides and emerges from the prism travelling parallel to its original direction but going the opposite way. (see Fig. 1).

A convex lens causes parallel rays of light to be bunched together or converged by refraction, whereas a concave lens cause such rays to diverge (see Fig. 1). The rays then meet on the other side of the lens at a focal point F or can be traced back to what appears to be a virtual focal point F' in front of the lens.

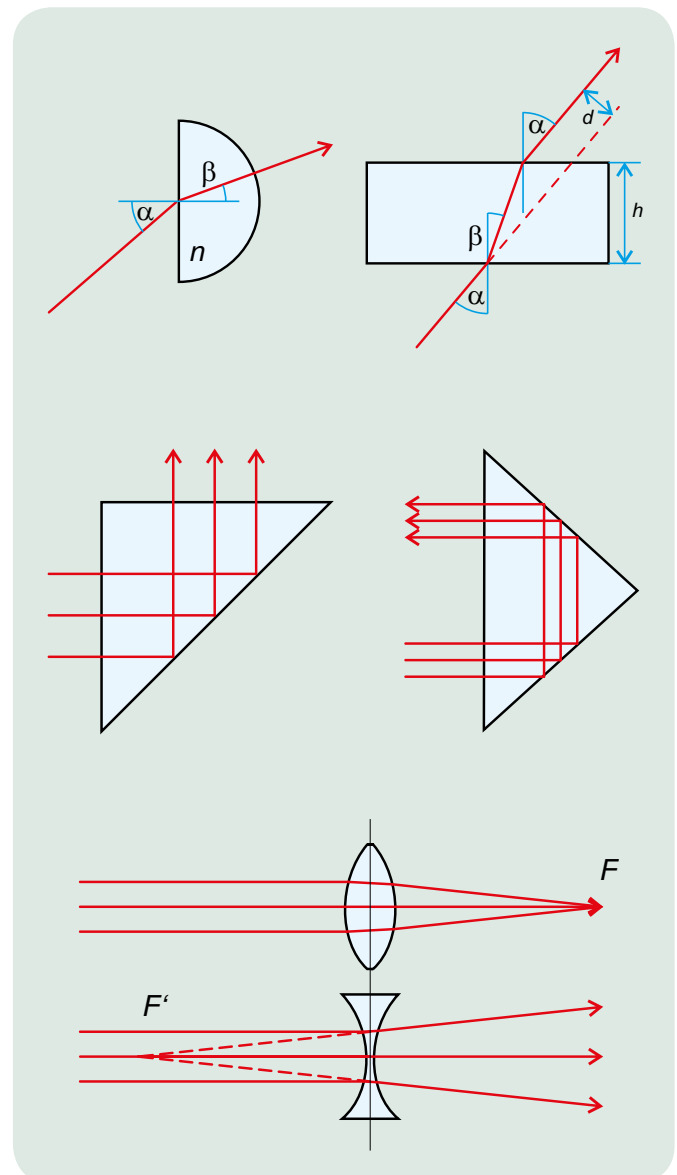


Fig. 1: Refraction by a semi-circular body, path of light through a rectangular block, deflecting and reversing prisms, path of light through a rectangular convex lens and through a concave lens

EVALUATION

If the original medium is air, for the purposes of this experiment it will be sufficiently accurate to assume that its refractive index $n_1 = 1$. If the angle of incidence is equal to the critical angle for total internal reflection α_c , the angle of refraction $\beta = 90^\circ$. From equation (2) it therefore follows that if n is the refractive index for transparent acrylic, then:

$$\sin \alpha_c = \frac{1}{n}$$

For refraction by a rectangular block, equations (2) and (3) imply the following:

$$d = h \cdot (\sin \alpha \cdot \cos \alpha \cdot \tan \beta) = h \cdot \sin \alpha \left(1 - \frac{\cos \alpha}{\sqrt{n^2 - \sin^2 \alpha}} \right)$$

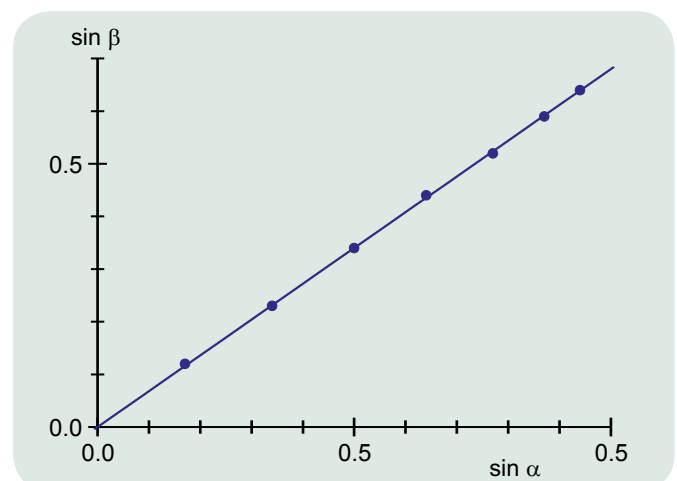
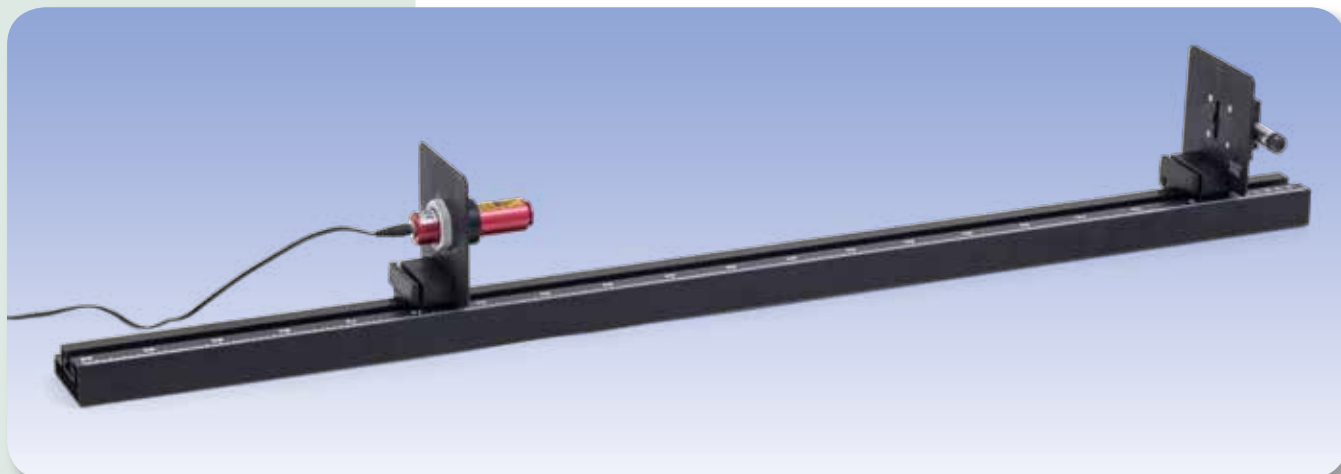


Fig. 2: Diagram for determination of refractive index n



EXPERIMENT PROCEDURE

- Investigate diffraction by single slits of various different widths.
- Investigate diffraction by a single slit for light of differing wavelengths.
- Investigate diffraction by a single slit and by an opaque object of the same size (Babinet's principle).

OBJECTIVE

Demonstrate the wave nature of light and determine the wavelength

SUMMARY

Diffraction of light by a single slit can be described as the superposition of coherent wavelets which, according to Huygens' principle, spread out from the illuminated slit in all directions. Depending on the angle along which they propagate, the wavelets cause either constructive or destructive interference. If the width of the slit and the distance to the screen are known, then the wavelength can be calculated based on the distance between adjacent dark bands of the interference pattern.

REQUIRED APPARATUS

Quantity	Description	Number
1	Laser Diode, Red	1003201
1	Laser Module, Green	1003202
1	Optical Bench K, 1000 mm	1009696
2	Optical Rider K	1000862
1	Adjustable Slit K	1008519
1	Holder K for Diode Laser	1000868

Additionally required

Wire



You can find technical information about the equipment at 3bscientific.com

1

BASIC PRINCIPLES

Diffraction of light by a single slit can be described as the superposition of coherent wavelets which, according to Huygens' principle, spread out from the illuminated slit in all directions. This superposition leads to either constructive or destructive interference depending on the angle. Beyond the slit a system of light and dark bands can be observed on a screen.

Where the wavelets cancel – i.e. where the bands are darkest – it can be seen that for every wavelet from one half of the slit there is another wavelet from the second half which interacts with it in such a way that the combined amplitude is reduced to a minimum. This happens when the path difference Δs_n between the beam through the middle of the slit and a ray from the edge is precisely an integer multiple n of half the wavelength λ :

$$(1) \quad \Delta s_n = n \cdot \frac{\lambda}{2} = \frac{b}{2} \cdot \sin \alpha_n$$

$n = 0, \pm 1, \pm 2, \dots$: Order of diffraction
 b : Width of slit,
 α_n : Angle of propagation

The regions of maximum darkness are symmetrical about the primary ray (see Fig. 1). Their distance from the primary ray, as measured in the plane of observation is as follows:

$$(2) \quad x_n = L \cdot \tan \alpha_n$$

L : Distance between slit and plane of observation

For a small angle, the following is therefore true:

$$(3) \quad \alpha_n = x_n = \frac{\lambda \cdot L}{b} \cdot n = \Delta \cdot n \quad \text{where} \quad \Delta = \frac{\lambda \cdot L}{b}$$

Δ : Relative distance between minima

A slit and an opaque obstruction of the same size and shape are considered complementary diffraction objects. According to Babinet's principle, the diffraction patterns of both objects, outside of the "unaffected" beam, are identical. The diffraction minima in both patterns are therefore in the same place.

In this experiment diffraction by single slits of various widths is investigated, along with diffraction of different wavelengths of light. Moreover, it will be shown that diffraction by a single slit and by an opaque object of the same width results in complementary diffraction patterns.

EVALUATION

The brightness is greatest in the direction of the primary ray. The value Δ can be determined as the gradient of the straight line graph when the distances x_n are plotted against n . Since Δ is obviously inversely proportional to the width of the slit b , the quotients Δ/L can be plotted in a graph against $1/b$ and the wavelength λ is then determined as the gradient of the graph of these measurements.

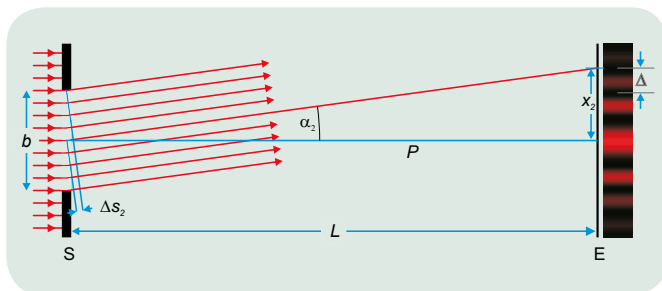


Fig. 1: Schematic diagram of diffraction of light by a single slit (S: Slit, b : Width of slit, E: Plane of observation, P : Primary beam, L : Distance of observation screen from slit, x_2 : Distance of second minimum from centre, α_2 : Direction of observation for second minimum, Δs_2 : Path difference between ray through centre and ray from edge).

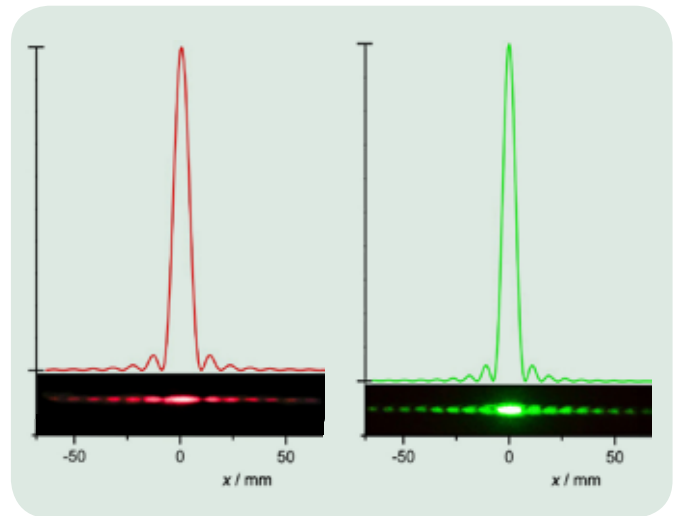


Fig. 2 Calculated and measured intensities for diffraction from a slit of width 0.3 mm with light of wavelength $\lambda = 650$ nm and $\lambda = 532$ nm.

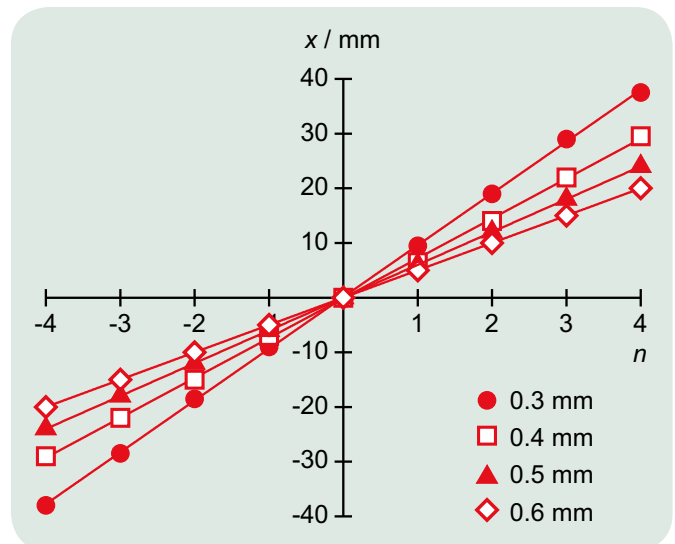


Fig. 3: Separations x_n as a function of diffraction order n for various widths of slit b where $\lambda = 650$ nm.

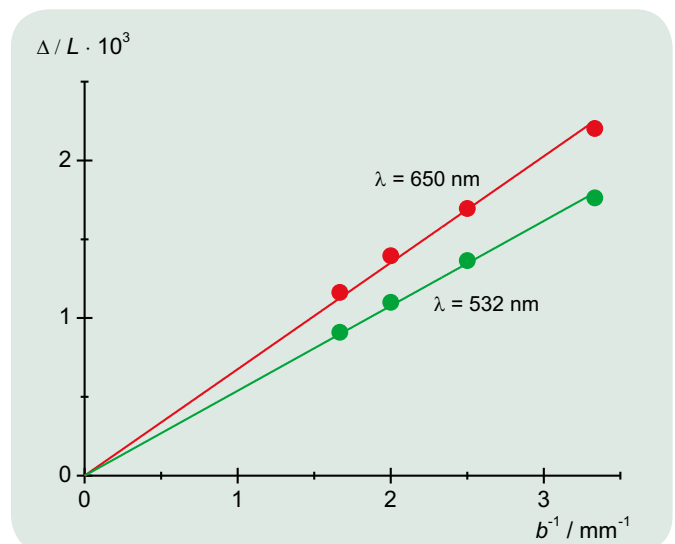
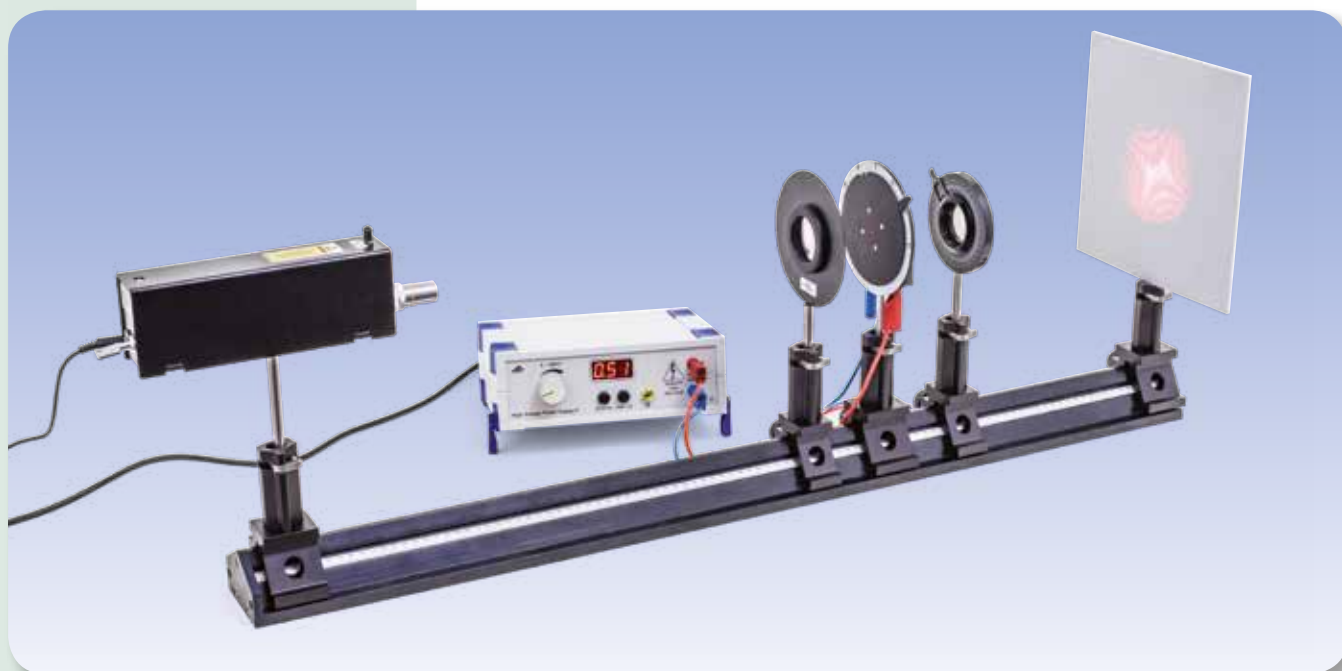


Fig. 4: Quotient of relative separation of minima Δ and distance L as a function of width of slit $1/b$.

UE4040500

POCKELS EFFECT



EXPERIMENT PROCEDURE

- Demonstrate birefringence in a conoscopic beam path.
- See how the birefringence changes when an electric field is applied.
- Determine the half-wave retardation voltage.



You can find technical information about the equipment at 3bscientific.com

2

OBJECTIVE

Demonstration of Pockels effect in a conoscopic beam path

SUMMARY

The Pockels effect is an electro-optical effect in which an electric field within a suitable material splits a light beam into two beams polarised perpendicular to one another. This ability to produce optical birefringence derives from the differing refractive indices depending on the direction of propagation and polarisation of the light. In the case of the Pockels effect, this increases linearly with the strength of the electric field as is demonstrated in this experiment using a lithium niobate crystal (LiNbO_3) placed in the path of a conoscopic beam. The interference pattern is formed by two sets of hyperbolae, from which the position of the optical axis for the birefringence can be seen directly.

REQUIRED APPARATUS

Quantity	Description	Number
1	Pockels Cell on Stem	1013393
1	Optical Precision Bench D, 100 cm	1002628
3	Optical Rider D, 90/50	1002635
2	Optical Rider D, 90/36	1012401
1	He-Ne Laser	1003165
1	Achromatic Objective 10x / 0.25	1005408
1	Polarisation Filter on Stem	1008668
1	Convex Lens on Stem $f = +50$ mm	1003022
1	Projection Screen	1000608
1	High-Voltage Power Supply E 5 kV (230 V, 50/60 Hz)	1013412 or
	High-Voltage Power Supply E 5 kV (115 V, 50/60 Hz)	1017725
1	Pair of Safety Experiment Leads, 75 cm	1002849

BASIC PRINCIPLES

The Pockels effect is an electro-optical effect in which an electric field within a suitable material splits a light beam into two beams polarised perpendicular to one another. This ability to produce optical birefringence derives from the differing refractive indices depending on the direction of propagation and polarisation of the light. In the case of the Pockels effect, this increases linearly with the strength of the electric field as is demonstrated in this experiment using a lithium niobate crystal (LiNbO₃) placed in the path of a conoscopic beam.

The crystal in this case is located inside a Pockels cell in transverse alignment, where an electric field is applied across the crystal in the direction of the optical axis for the birefringence (see Fig. 1). The light beam passing perpendicularly through the crystal splits into an ordinary and an extraordinary, i.e. one polarised in the direction of the optical axis for the birefringence and another polarised perpendicular to it. In the case of lithium niobate, the refractive index for the ordinary beam for $n_o = 2.29$ as measured at the wavelength of an He-Ne laser $\lambda = 632.8$ nm while that for the extraordinary beam is $n_e = 2.20$. The path difference between the ordinary and extraordinary beams is as follows:

$$(1) \quad \Delta = d \cdot (n_o - n_e),$$

where $d = 20$ mm, the thickness of the crystal in the direction of the beam.

Demonstration of the birefringence uses a classical beam path as suggested for the purpose in numerous optics text books. The crystal is illuminated by a divergent, linearly polarised light beam and the transmitted light is observed behind an orthogonal analyser. The optical axis of the birefringence is highly visible in the interference pattern since it stands out from the background due to its symmetry. In this experiment, it is parallel to the entry and exit surfaces on the crystal, therefore creating an interference pattern with two sets of hyperbolae rotated by 90° with respect to one another. The actual axis of the first set of hyperbolae is parallel to the optical axis of the birefringence and that of the second set is perpendicular to it.

The dark bands in the sets of hyperbolae arise for beams where the difference between the optical paths of the ordinary and extraordinary beams in the crystal are an integer multiple of the wavelength. These beams retain their original linear polarisation on passing through the crystal and get blocked by the analyser.

The path difference corresponds to about 2800 wavelengths of the laser light being used. However, in general Δ is not precisely an integer multiple of the wavelength λ , but rather lies between two values $\Delta_m = m \cdot \lambda$ and $\Delta_{m+1} = (m + 1) \cdot \lambda$. For the dark lines of the first set of hyperbolae the path differences are Δ_{m+1} , Δ_{m+2} , Δ_{m+3} , etc. Those for the second set correspond to Δ_m , Δ_{m-1} , Δ_{m-2} , etc. (see Fig. 2). The position of the dark bands, or more accurately their distance from the centre, depends on the difference between Δ and $m \cdot \lambda$. The Pockels effect increases or decreases the difference between the primary refractive indices $n_o - n_e$ depending on the sign of the voltage applied. This means that the difference $\Delta - m \cdot \lambda$ changes and so therefore does the position of the dark interference bands. If the so-called half-wave retardation voltage U_{π} is applied, then Δ changes by one half of the wavelength. Then the dark interference bands shift to the position of the bright bands and vice versa. This process is repeated every time the voltage is increased by U_{π} .

EVALUATION

For a voltage U_1 the dark interference bands of order +1 are located precisely in the centre. For the next voltage U_2 it is those of order +2 which are in the centre. Then the half-wave voltage is as follows:

$$U_{\pi} = \frac{U_2 - U_1}{2}$$

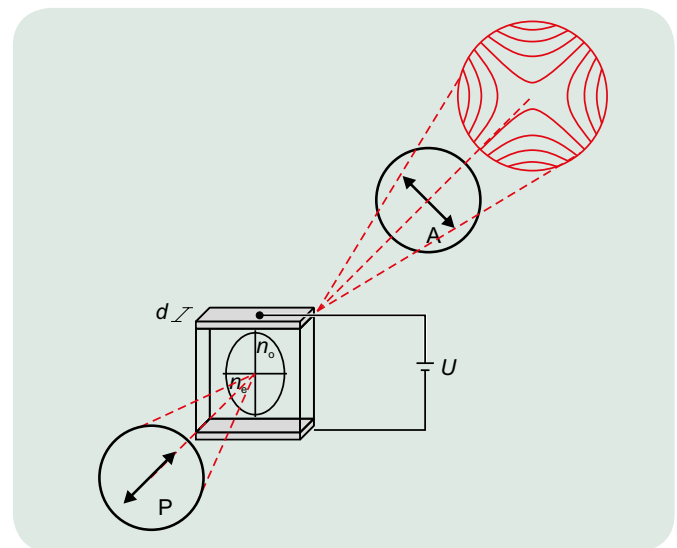


Fig. 1: Schematic of Pockels cell in a conoscopic beam path between the polariser and analyser

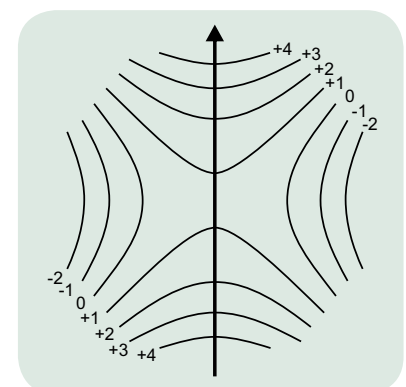


Fig. 2: Interference pattern with optical axis of crystal in the direction of the arrow. The indices of the dark interference bands indicate the path difference between the ordinary and extraordinary beams in units of the wavelength.

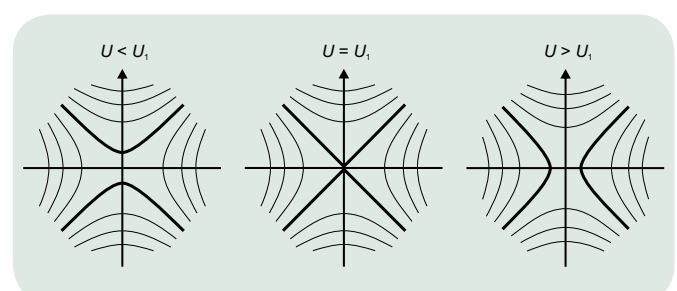


Fig. 3: Change in interference pattern due to Pockels effect. The hyperbolae indicated by thicker lines are those of order +1 in the interference pattern.



OBJECTIVE

Set up and calibrate a prism spectrometer

SUMMARY

A prism spectrometer utilises the dispersion of light into its spectral components by means of a prism to measure optical spectra. In order to measure wavelengths, it is necessary to calibrate the system since the angular dispersion is non-linear. In this experiment the known spectrum of a mercury (Hg) lamp will be used for calibration purposes and then measurements will be made for a cadmium (Cd) lamp.

EXPERIMENT PROCEDURE

- Make adjustments to a prism spectrometer and calibrate it using the spectral lines from a mercury lamp.
- Measure the minimum angle of deflection when $\lambda = 546.07 \text{ nm}$.
- Determine the refractive index of flint glass when $\lambda = 546.07 \text{ nm}$ and the Cauchy parameters b and c for the wavelength-dependent refractive index.
- Calculate a calibration curve according to the Hartmann dispersion formula.
- Make measurements on an unknown line spectrum.



You can find technical information about the equipment at 3bscientific.com

2

REQUIRED APPARATUS

Quantity	Description	Number
1	Spectrometer-Goniometer	1002912
1	Control Unit for Spectrum Lamps (230 V, 50/60 Hz)	1003196 or
	Control Unit for Spectrum Lamps (115 V, 50/60 Hz)	1003195
1	Spectral Lamp Hg/Cd	1003546
1	Spectral Lamp Hg 100	1003545

BASIC PRINCIPLES

Prism spectrometers are used to measure optical spectra using the dispersion of light into its spectral components when it passes through a prism. This dispersion results from the fact that the refractive index is dependent on wavelength. It is non-linear and therefore the prism spectrometer needs to be calibrated in order to measure wavelengths.

Inside the spectrometer, the light being investigated passes through slit S to strike the objective O_1 . These two components form a collimator and produce a wide, parallel beam of light (see Fig. 1). After refracting at two surfaces of the prism, a parallel beam exits the prism and is focussed to an image of the slit in the focal plane of objective O_2 . This can then be viewed via the ocular lens OC. The telescope formed by objective O_2 and ocular OC is attached to a swivelling arm which is rigidly connected to the vernier scale N.

The double refraction of the light by the prism can be described by the angles α_1 , α_2 , β_1 and β_2 (see Fig. 2). The following relationships are true for an equilateral prism:

$$(1) \quad \sin \alpha_1 = n(\lambda) \cdot \sin \beta_1(\lambda), \quad n(\lambda) \cdot \sin \beta_2(\lambda) = \sin \alpha_2(\lambda), \quad \beta_1(\lambda) + \beta_2(\lambda) = 60^\circ.$$

The angle of incidence α_1 can be altered by turning the prism with respect to the parallel beam which enters it. Angles α_2 , β_1 and β_2 are dependent on the wavelength λ since the refractive index n is wavelength-dependent.

The angle of deflection between the collimator and the telescope is determined from the angle of incidence α_1 and the exit angle α_2 :

$$(2) \quad \delta(\lambda) = \alpha_1 + \alpha_2(\lambda) - 60^\circ.$$

The angle is at its minimum δ_{\min} , when the path of the beam is symmetrical with respect to the prism. At the same time the angular dispersion $d\delta/d\lambda$ will be at its maximum. Prism spectrometers are

therefore adjusted in such a way that a symmetrical beam path is attained for a reference wavelength λ_0 . In this experiment, the green spectral line ($\lambda_0 = 546.07 \text{ nm}$) of a mercury lamp is chosen for this. The refractive index of the prism at the reference wavelength can be determined from the minimum angle of deflection. This is because the symmetry implies that $\beta_1(\lambda_0) = \beta_2(\lambda_0) = 30^\circ$ and $\alpha_2(\lambda_0) = \alpha_1$, therefore:

$$(3) \quad \sin \alpha_1 = n(\lambda_0) \cdot \frac{1}{2} \quad \text{where} \quad \alpha_1 = \frac{\delta_{\min}}{2} + 30^\circ.$$

The dispersion means that the other spectral lines are shifted from δ_{\min} by small angles $\Delta\delta$. You will be able to read off these angles to an accuracy of minutes using the vernier scale. Since the changes in refractive index Δn remain small over the entire visible part of the spectrum, it is sufficient to consider only the linear terms in the changes. Therefore from equations 1 – 3 the following relationship can be derived between the wavelengths and deflection:

$$(4) \quad \Delta\delta(\lambda) = \Delta\alpha_2(\lambda) = \frac{\Delta n(\lambda)}{\cos \alpha_1} = \frac{\Delta n(\lambda)}{\sqrt{1 - \frac{(n(\lambda_0))^2}{4}}}.$$

In the visible part of the spectrum, the refractive index n decreases as the wavelength λ increases. This can be described by the Cauchy equation in the following form:

$$(5) \quad n(\lambda) = a + \frac{b}{\lambda^2} + \frac{c}{\lambda^4}.$$

In principle, it is possible to obtain a mathematical description for a calibration curve from equations (4) and (5). However, the Hartmann dispersion formula turns out to be better suited to the purpose.

$$(6) \quad \delta(\lambda) = \delta_H + \frac{K}{\lambda - \lambda_H}$$

The modifying parameters δ_H , K and λ_H in the above do not, however, have any specific physical meaning.

For this reason, in the experiment the spectral lines of the mercury lamp are utilised for calibration purposes with the help of equation (6) and afterwards the lines of an “unknown” spectrum will be measured (see Table 1).

EVALUATION

The refractive index $n(\lambda_0)$ is given from equation 3 The Cauchy parameters for the refractive index can be calculated by fitting a parabolic curve to the equation $\Delta n = n(\lambda) - n(\lambda_0) = f(1/\lambda^2)$.

Table1: Wavelengths of lines in Cd spectrum

Colour	Measurement λ / nm	Table value λ / nm
Blue (medium deflection)	466	466
Blue (large deflection)	468	468
Cyan (medium deflection)	479	480
Dark green (large deflection)	509	509
Dark green (less deflection)	515	516
Red (large deflection)	649	644

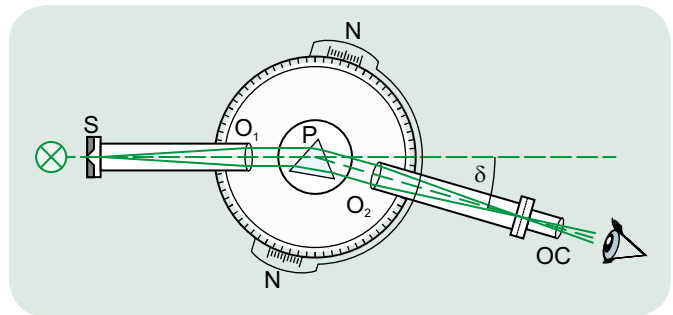


Fig. 1: Schematic of a prism spectrometer

S: Entry slit, O₁: Collimator objective, P: Prism, O₂: Telescope objective, OC: Telescope eyepiece (ocular), δ : Angle of deflection

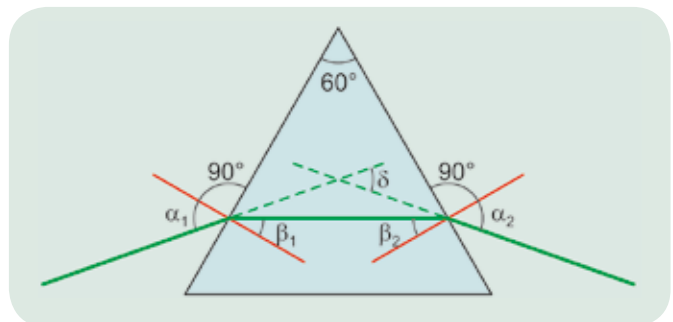


Fig. 2: Beam path through prism

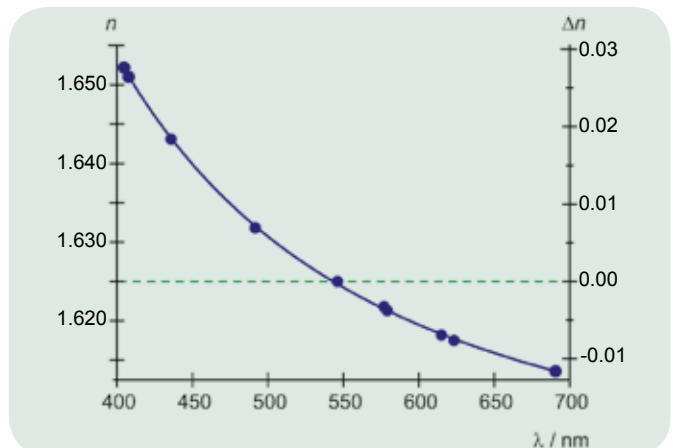


Fig. 3: Wavelength-dependent refractive index for flint glass prism

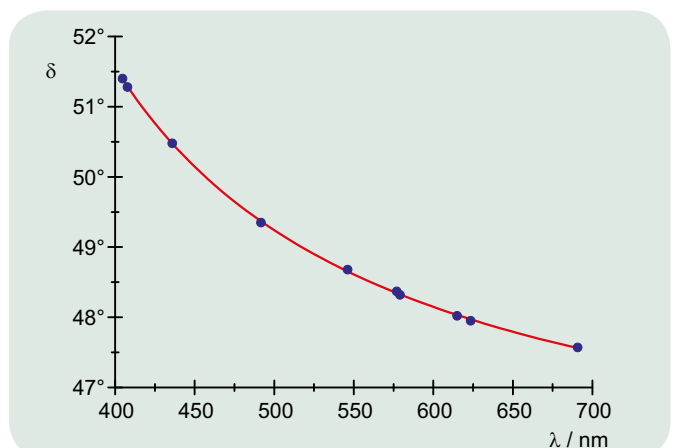


Fig. 4: Calibration curve for prism spectrometer

UE5010400

MILLIKAN'S EXPERIMENT



OBJECTIVE

Carry out Millikan's experiment to confirm the value of the elementary charge with the help of charged oil drops

SUMMARY

Between the years 1910 and 1913, *Robert Andrews Millikan* managed to measure the elementary electric charge to an unprecedented accuracy and thereby confirmed the quantum nature of charge. The experiment which now bears his name is based on measuring the quantity of charge carried by charged drops of oil, which are able to rise through the air

under the influence of an electric field from a plate capacitor and descend when the field is absent. The Millikan apparatus used for this version of the experiment utilises a compact piece of equipment which is based on Millikan's design and which does not require any radioactive source.

EXPERIMENT PROCEDURE

- Produce and select suitable oil drops and observe them in an electric field.
- Measure the speed with which they rise in the electric field and descend without it.
- Confirm the value of the elementary charge.



You can find technical information about the equipment at 3bscientific.com

2

REQUIRED APPARATUS

Quantity	Description	Number
1	Millikan's Apparatus (230 V, 50/60 Hz)	1018884 or
	Millikan's Apparatus (115 V, 50/60 Hz)	1018882

BASIC PRINCIPLES

Between the years 1910 and 1913, *Robert Andrews Millikan* managed to measure the elementary electric charge to an unprecedented accuracy and thereby confirmed the quantum nature of charge. He was awarded the Nobel Prize in physics for his work. The experiment which now bears his name is based on measuring the quantity of charge carried by charged drops of oil, which are able to rise through the air under the influence of an electric field from a plate capacitor and descend when the field is absent. The value he obtained for the elementary charge $e = (1.592 \pm 0.003) \cdot 10^{-19}$ C differs by only 0.6% from the accepted modern value.

The forces which act on a droplet of oil (which we shall assume to be spherical) situated in the electric field of a plate capacitor are:

the force of gravity,

$$(1) \quad F_G = m_2 \cdot g = \frac{4}{3} \cdot \pi \cdot r_0^3 \cdot \rho_2 \cdot g,$$

m_2 : Mass of oil drop, r_0 : Radius of oil drop, ρ_2 : Density of oil, g : Acceleration due to gravity

the drop's buoyancy in air,

$$(2) \quad F_A = \frac{4}{3} \cdot \pi \cdot r_0^3 \cdot \rho_1 \cdot g,$$

ρ_1 : Density of air

the force exerted by the electric field E ,

$$(3) \quad F_E = q_0 \cdot E = \frac{q_0 \cdot U}{d},$$

q_0 : Charge on oil drop, U : Voltage between the plates of the capacitor,
 d : Separation of the capacitor plates

and Stokes' force of friction

$$(4) \quad F_{R1,2} = 6 \cdot \pi \cdot \eta \cdot r_0 \cdot v_{1,2}.$$

η : Viscosity of air, v_1 : Speed of ascent, v_2 : Speed of descent

When an oil drop rises in an electric field, the equilibrium equation involves the following forces:

$$(5) \quad F_G + F_{R1} = F_E + F_A$$

During descent the equation is as follows:

$$(6) \quad F_G = F_{R2} + F_A.$$

This means we can find the radius of the drop and its charge:

$$(7) \quad r_0 = \sqrt{\frac{9}{2} \cdot \frac{\eta \cdot v_2}{(\rho_2 - \rho_1) \cdot g}}$$

and

$$(8) \quad q_0 = \frac{6 \cdot \pi \cdot \eta \cdot d \cdot (v_1 + v_2)}{U} \cdot r_0.$$

Very small radii r_0 are of the same order of magnitude as the mean free path of air molecules. This means a correction needs to be made to the Stokes' friction. The corrected radius r and charge q are then given by the following:

$$(9) \quad r = \sqrt{r_0^2 + \frac{A^2}{4}} - \frac{A}{2} \quad \text{where } A = \frac{b}{p}$$

$b = 82 \mu\text{m} \cdot \text{hPa} = \text{constant}$, p : Air pressure

$$(10) \quad q = q_0 \cdot \left(1 + \frac{A}{r}\right)^{-1.5}.$$

The Millikan apparatus used for this version of the experiment uses a compact piece of equipment which is based on Millikan's design and which does not require any radioactive source. The charged oil drops are produced with the help of an atomiser, after which the random charge they assume is no longer affected by external influences. As in Millikan's own set-up, the droplets are introduced into the experiment chamber from above. Suitable oil drops are selected and their charge determined by observing them through a measuring microscope. For each of the drops chosen, the time to rise a certain distance in the electric field is measured, as is the time it takes to descend by the same distance with the field absent. The distance is taken to be that between two adjacent scale markings on the ocular. The polarity of the capacitor plates is selected in accordance with the sign of the charge. An alternative is to apply a field sufficient to cause the drops being measured to hover stationary in one place.

The times measured for ascent and descent of a charged drop, the voltage applied across the plates and the other parameters relevant to evaluating the results, temperature, viscosity and pressure are displayed on the touch-sensitive screen.

EVALUATION

The speeds of ascent and descent are obtained from the times t_1 and t_2 measured for the ascent or descent to occur:

$$v_{1,2} = \frac{s}{V \cdot t_{1,2}},$$

s : Distance between two selected markings on the ocular scale,

$V = 2$: Objective magnification

From these the charge q on the oil drop is calculated using equation (10). The charges q_i determined from these measurements (Table 1) are all divided by a whole number n_i in such a way that the resulting values exhibit a minimum of variation about the mean value. The degree of spread about the mean is indicated by the standard deviation. The best estimate for elementary charge e and the standard deviation Δe can be determined from the values e_i obtained from individual measurements along with their individual deviations from the mean Δe_i (Table 1) by forming a weighted mean as below:

$$e \pm \Delta e = \frac{\sum w_i \cdot e_i}{\sum w_i} \pm \frac{1}{\sqrt{\sum w_i}} \quad \text{where } w_i = \left(\frac{1}{\Delta e_i}\right)^2.$$

Using the values from Table 1, this results in:

$$e \pm \Delta e = \frac{1286}{799} \pm \frac{1}{28} = (1.61 \pm 0.04) \cdot 10^{-19} \text{ C}.$$

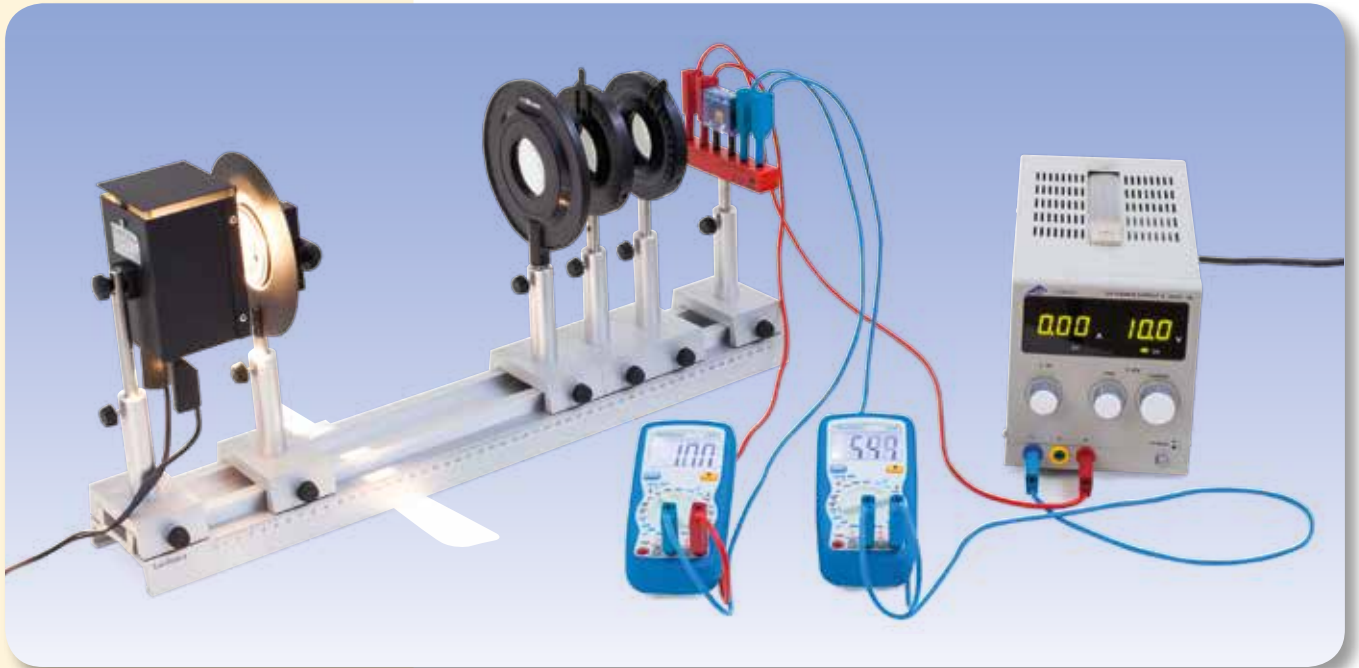
The result is therefore all the more significant, the greater the number of measurements that are made, i.e. the larger the quantity of samples and the smaller the number n of differing charges on the drops. Due to measurement uncertainties, particularly in the distance between capacitor plates and readings from the microscope scale, it would be expected that $n \leq 7$.

Table 1: Charges q_i measured for ten different oil drops and the value e_i determined for the elementary charge.

i	Polarity	q_i 10^{-19} C	Δq_i 10^{-19} C	n	e_i 10^{-19} C	Δe_i 10^{-19} C
1		-11.1	0.9	-7	1.59	0.13
2		-7.9	0.6	-5	1.58	0.12
3		-6.2	0.4	-4	1.55	0.10
4		3.5	0.2	2	1.75	0.10
5		4.9	0.3	3	1.63	0.10
6		6.3	0.5	4	1.58	0.13
7		6.6	0.4	4	1.65	0.10
8		7.6	0.6	5	1.52	0.12
9		10.2	0.8	6	1.70	0.13
10		10.6	0.8	7	1.51	0.11

UE6020400

PHOTOCONDUCTIVITY



**EXPERIMENT
PROCEDURE**

- Measure current as a function of voltage for various intensities of light.
- Measure current as a function of light intensity for various voltages.

OBJECTIVE

Record the characteristic curve for a photoresistor

SUMMARY

Photoconductivity utilises absorption of light by means of the inherent photoelectric effect in a semiconductor to create electron-hole pairs. One specific semiconductor mix which exhibits the photoelectric effect particularly strongly is cadmium sulphide. This material is used in the construction of photoresistors. In this experiment, a CdS photoresistor is illuminated with white light from an incandescent bulb. The intensity of this illumination of the photoresistor is then varied by crossing two polarising filters placed one behind the other in the beam.

REQUIRED APPARATUS

Quantity	Description	Number
1	Optical Bench U, 600 mm	1003040
6	Optical Rider U, 75 mm	1003041
1	Experimental Lamp, Halogen	1003038
1	Adjustable Slit on Stem	1000856
1	Convex Lens on Stem $f = +150$ mm	1003024
2	Polarisation Filter on Stem	1008668
1	Holder for Plug-in Components	1018449
1	DC Power Supply 0 – 20 V, 0 – 5 A (230 V, 50/60 Hz)	1003312 or
	DC Power Supply 0 – 20 V, 0 – 5 A (115 V, 50/60 Hz)	1003311
2	Digital Multimeter P1035	1002781
3	Pair of Safety Experimental Leads, 75 cm, red/blue	1017718



You can find technical information about the equipment at 3bscientific.com

2

BASIC PRINCIPLES

Photoconductivity utilises absorption of light by means of the photoelectric effect in a semiconductor to create electron-hole pairs. In some semiconductors, this effect is dominated by boundaries of discontinuities in the material. The effect is then not only dependent on the basic material, but also on its microstructure and on impurities. Ionisation of these impurities acts in a similar way to doping for a few milliseconds, increasing the electrical conductivity of the material. One specific semiconductor mix which exhibits the inherent photoelectric effect particularly strongly is cadmium sulphide, which is used to make photoresistors.

Absorption increases the conductivity of the semiconductor in a manner described by the following equation:

$$(1) \quad \Delta\sigma = \Delta p \cdot e \cdot \mu_p + \Delta n \cdot e \cdot \mu_n$$

e : Elementary charge,

Δn : Change in electron concentration, Δp : Change in hole concentration,
 μ_n : Electron mobility, μ_p : Hole mobility

When a voltage U is applied, the photoelectric current is given by the following:

$$(2) \quad I_{ph} = U \cdot \Delta\sigma \cdot \frac{A}{d}$$

A : Cross-section of current path,
 d : Length of current path

The semiconductor therefore acts in a circuit like a light-dependent resistor, the value of its resistance decreasing when light shines upon it. The dependence of current on light intensity Φ at a constant voltage may be expressed in the form

$$(3) \quad I_{ph} = a \cdot \Phi^\gamma \text{ where } \gamma \leq 1.$$

Here the value γ is indicative of the recombining processes within the semiconductor material.

In this experiment, a CdS photoresistor is illuminated with white light from an incandescent bulb. Measurements are made of how current I through a CdS photoresistor depends on the applied voltage U at constant light intensity Φ and how it depends on intensity Φ at constant voltage U . The intensity is varied by crossing two polarising filters placed one behind the other in the light beam.

If the maximum power dissipation of 0.2 W is exceeded, the photoresistor will be damaged. For this reason the intensity of the incident light in the experiment is limited by means of an adjustable slit directly behind the light source.

EVALUATION

The current-voltage characteristics of a CdS photoresistor are along a straight line through the origin, as implied by equation (2).

In order to describe the characteristics for current and light intensity, the term $\cos^2\alpha$ is calculated for use as a relative measure of light intensity. In this case, α is the angle between the directions of polarisation of the two filters. However, even when they are fully crossed, the filters will not block all the light. Also, it is not possible to avoid entirely the intrusion of residual light from the room in which the experiment is taking place. Under such circumstances, equation (3) needs to be modified to

$$I = a \cdot \Phi^\gamma + b \text{ with } \gamma \leq 1.$$

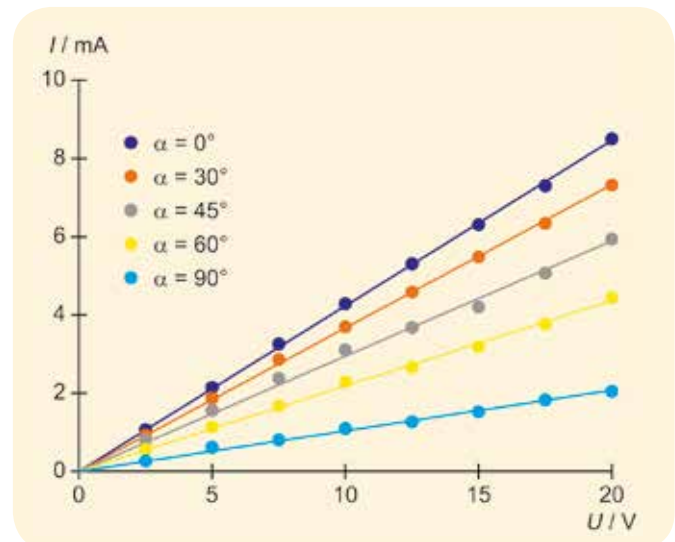


Fig. 1: Current-voltage characteristics of a CdS photoresistor for various intensities of light.

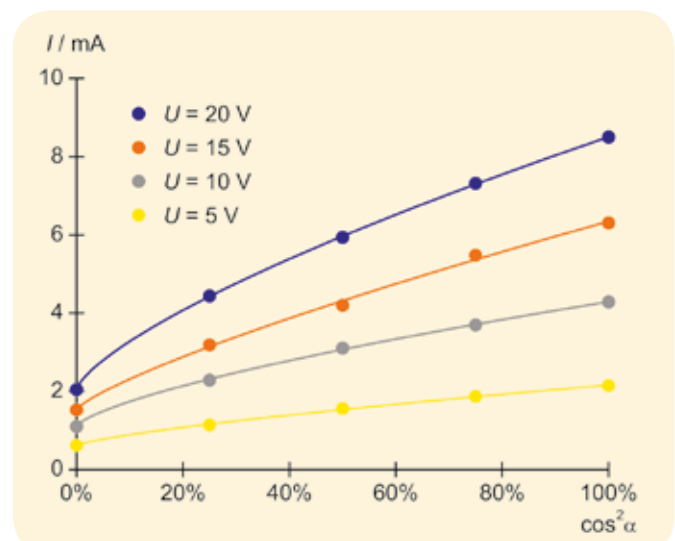


Fig. 2: Characteristics for current and light intensity of a CdS photoresistor at various voltages.

**OBJECTIVE**

Record the characteristics of a photovoltaic module (solar cell) as a function of the luminosity

EXPERIMENT PROCEDURE

- Measuring the $I-U$ characteristics of a photovoltaic module (solar cell) at various illumination levels.
- Comparing the measured characteristics with a calculation in accordance with the single-diode model.
- Determining the relationship between the no-load voltage and the short-circuit current for various illumination levels.

SUMMARY

A photovoltaic system converts light energy from sunlight to electrical energy. To do this, solar cells are used which are comprised of, for example, suitably doped silicon and consequently correspond to an up-scaled photodiode. Light absorbed by the solar cell releases charge carriers from their crystal bonds which result in a photoelectric current flowing opposite the forward direction of the p-n junction. It is the diode current of the solar cell that limits current output to an external load. When at the so-called no-load or idle voltage U_{OC} , this current reaches a zero value because the photoelectric current and the diode current precisely offset each other and only becomes negative when a voltage is applied that is above the no-load voltage. When a positive current range is reached, the solar cell can be operated as a generator that outputs electrical power to an external load. In the experiment, the voltage-current characteristics of this generator are measured as a function of the illumination level and described with a set of simple parameters.

REQUIRED APPARATUS

Quantity	Description	Number
1	SEK Solar Energy (230 V, 50/60 Hz)	1017732 or
	SEK Solar Energy (115 V, 50/60 Hz)	1017731
1	DC Power Supply 0 – 20 V, 0 – 5 A (230 V, 50/60 Hz)	1003312 or
	DC Power Supply 0 – 20 V, 0 – 5 A (115 V, 50/60 Hz)	1003311

BASIC PRINCIPLES

The term photovoltaic is a combination of the Greek work phos (light) and the Italian name Volta. This is in honour of *Alessandro Volta*, who, among other things, invented the first functional electrochemical battery. A photovoltaic system converts limitlessly available and free light energy from sunlight into electrical energy without causing any CO₂ emissions. To do this solar cells are needed, which in most cases are made of suitably doped silicon and thus corresponds to a scaled-up photodiode. Prior to reaching the external contacts of the solar cell, first the light absorbed by the solar cell releases charge carriers from their crystal bonds (internal photoeffect), due to the electrical field achieved through suitable dosing of the p-n junction the electrons drift to the n-doped side and the holes drift to the p-doped side (Fig. 1). This is how a photoelectric current arising flows in the reverse direction to the forward direction of the p-n junction, which can output the electrical power to an external load.



You can find technical information about the equipment at 3bscientific.com

1

The photoelectric current I_{ph} is proportional to the illumination level Φ :

$$(1) \quad I_{ph} = \text{const} \cdot \Phi$$

It is superpositioned by the diode current in the forward or conducting direction:

$$(2) \quad I_D = I_S \cdot \left(\exp\left(\frac{U}{U_T}\right) - 1 \right)$$

I_S : Saturation current, U_T : Temperature voltage

and grows ever stronger the more voltage U between the contacts exceeds the diffusion voltage U_D . Thus the current I output available for external loads is limited by the diode current:

$$(3) \quad I = I_{ph} - I_D = I_{ph} - I_S \cdot \left(\exp\left(\frac{U}{U_T}\right) - 1 \right)$$

It reaches the value zero for so-called no-load or idle voltage U_{OC} because the photo-electric current and the diode current mutually offset each other and only becomes negative if a voltage $U > U_{OC}$ is applied.

In the range of positive currents the solar cell can be operated as a generator to output electrical energy to an external load. Eq. (3) expresses the $I-U$ characteristic of this generator. Since in actual practice the photo-electric current I_{ph} is considerably higher than the saturation current I_S , we can derive from (3) the following relationship for the idle voltage:

$$(4) \quad U_{OC} = U_T \cdot \ln\left(\frac{I_{ph}}{I_S}\right)$$

If the terminals of solar cell are short-circuited, the cell supplies the short-circuit current I_{SC} , which corresponds to the photo-electric current since $U = 0$ according to Equation (3). Consequently, we obtain:

$$(5) \quad U_{OC} = U_T \cdot \ln\left(\frac{I_{SC}}{I_S}\right) \text{ where } I_{SC} = I_{ph}$$

Eq. 2 describes the diode response within the framework of the so-called standard model. Here the saturation current I_S happens to be a material variable, which depends on the geometrical and electrical data of the solar cell. For the temperature voltage U_T , the following holds true:

$$(6) \quad U_T = \frac{m \cdot k \cdot T}{e}$$

$m = 1 \dots 2$: Ideal factor

k : Boltzmann's constant, e : Elementary charge,

T : Temperature in Kelvin

In a more precise examination of the characteristic, leakage currents at the edges of the solar cells and point-like short-circuits of the p-n junction would be taken into consideration, which can be modelled using a parallel resistance R_p . Eq. 3 then becomes

$$(7) \quad I = I_{ph} - I_S \cdot \left(\exp\left(\frac{U}{U_T}\right) - 1 \right) - \frac{U}{R_p}$$

So in order to achieve effectively utilisable voltages in the range between 20 and 50 V, in practice we see a significant number of solar cells connected in series. Such a series connection configuration comprised of 18 solar cells is illuminated in the experiment using a halogen lamp of variable luminosity and the current-voltage characteristics of the module are recorded at varying luminosities.

EVALUATION

The family of current-voltage characteristics from the photovoltaic module (Fig. 2) can be described using Equation 7, if regardless of the luminosity the same set of parameters i.e. I_S , U_T and R_p is inserted and the photo-electric current I_{PH} is selected as a function of the luminosity. Of course the temperature voltage is the 18 times the value estimated in Eq. 6 because the module consists of 18 solar cells connected in series. A parallel circuit comprised of an ideal power source, a series connection of 18 semi-conductor diodes and an ohmic resistor, see Fig. 3 is provided as an equivalent circuit diagram for the photovoltaic module. The power source supplies a luminosity-dependent current in the reverse direction.

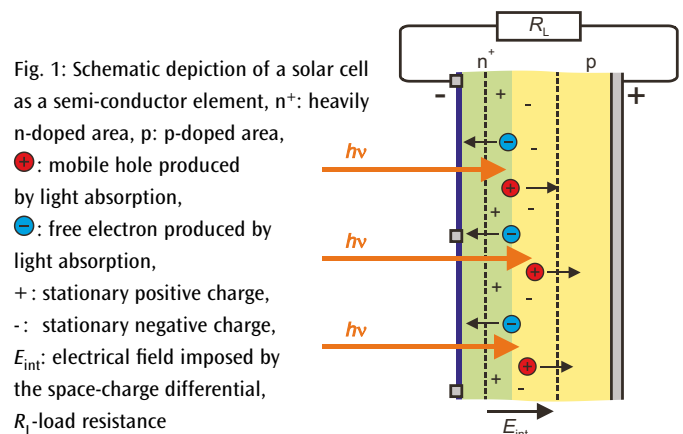


Fig. 1: Schematic depiction of a solar cell as a semi-conductor element, n⁺: heavily n-doped area, p: p-doped area, ●: mobile hole produced by light absorption, ●: free electron produced by light absorption, +: stationary positive charge, -: stationary negative charge, E_{int} : electrical field imposed by the space-charge differential, R_L -load resistance

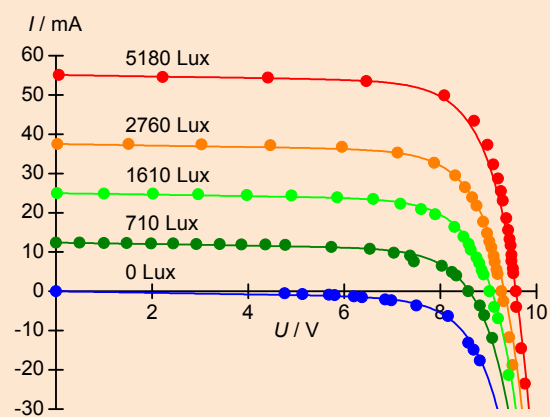


Fig. 2: Current-voltage family of characteristics of a photovoltaic module for five different luminosities

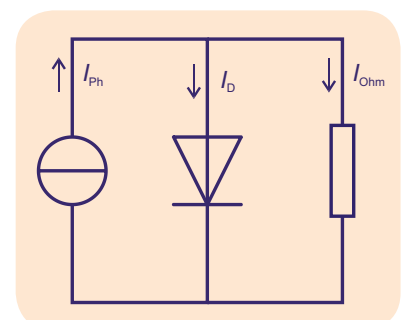


Fig. 3: Equivalent circuit diagram for the photovoltaic module

**OBJECTIVE**

Investigate how partial shading affects photovoltaic systems

EXPERIMENT PROCEDURE

- Measure and analyse the $I-U$ characteristic and $P-R$ characteristic for a series circuit containing two photovoltaic modules.
- Measure and analyse the characteristics with the modules partially in shade both with and without by-pass diodes.
- Demonstrate the reverse bias voltage for an unprotected module in shadow.
- Determine the loss of power resulting from partial shading.



You can find technical information about the equipment at 3bscientific.com

1**SUMMARY**

In photovoltaic installations, multiple solar modules are usually connected in series in a long line. The modules themselves are made up of many solar cells connected in series. In practice, it is possible for such systems to be partially in shadow. Individual parts of the system are then exposed to less light and therefore generate little current, which then limits the current in the whole series circuit. This can be avoided by means of by-pass diodes. In this experiment, two modules each consisting of 18 solar cells are formed into a simple photovoltaic system. They can optionally be connected in series with or without by-pass diodes and are then illuminated with light from a halogen lamp.

REQUIRED APPARATUS

Quantity	Description	Number
1	SEK Solar Energy (230 V, 50/60 Hz)	1017732 or
	SEK Solar Energy (115 V, 50/60 Hz)	1017731

BASIC PRINCIPLES

In photovoltaic installations, multiple solar modules are usually connected in series in a long line. The modules themselves are made up of many solar cells connected in series.

Calculation of current and voltage for such a series circuit follows from Kirchhoff's laws, taking into account the current-voltage characteristic of the solar cells. The same current I flows through all the modules in the series circuit and the voltage is given by

$$(1) \quad U = \sum_{i=1}^n U_i$$

n : Number of modules

This is the sum of all the voltages U_i between the terminals of the individual modules.

The current-voltage characteristic of a solar cell or module can be easily explained by means of an equivalent circuit diagram made up of a constant voltage source supplying a photoelectric voltage and a "semiconductor diode" connected in parallel with it but in reverse-bias direction. Resistive losses which occur are represented by a resistor, also connected in parallel in the system (see Experiment UE8020100 and Fig. 1). The photoelectric current is proportional to the intensity of the illuminating light. When the intensity is the same for all modules, then they all respond alike and individually supply the same voltage. Equation 1 then implies:

(2) $U = n \cdot U_1$

In practice, however, it is possible for such systems to be partially in shadow. Individual modules in the system are then exposed to less light and therefore generate little photoelectric current, which then limits the current in the whole series circuit. This limiting of current causes differing voltages U_i to be generated by the individual modules.

In the extreme case, the voltages across fully illuminated modules, even under short-circuit conditions ($U = 0$), can attain values going as far as the open-circuit voltage, see Fig. 2. The sum of these voltages is in reverse-bias direction across the modules in shadow. This can lead to enormous amounts of heating and can destroy the capsules in which the solar cells are contained or even the cells themselves. To protect against this, photovoltaic systems are equipped with by-pass diodes, which allow the current to by-pass elements which are in shadow.

In this experiment, two modules each consisting of 18 solar cells are formed into a simple photovoltaic system. They can optionally be connected with or without by-pass diodes in series and are then illuminated with light from a halogen lamp. Initially the two modules are both illuminated with the same bright intensity of light, but later one module is put into shadow such that it only supplies half the amount of current.

In all cases I - U characteristics are plotted from short-circuit to open-circuit range and compared. Power values are also calculated as a function of the load resistance to determine the amount of power loss as a result of the shading and to determine the effect of the by-pass diodes.

For the case of a short-circuit, the voltage across the shaded module is also measured separately. It reaches -9 V if the module is not protected by a by-pass diode.

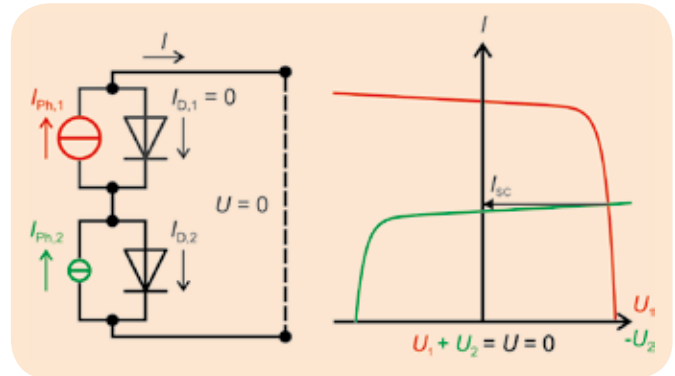


Fig. 2: Schematic diagram of partial shading of two modules with no by-pass diodes under short-circuit conditions ($U = 0$). The characteristic of the shaded model (green) is shown reversed. Here it represents a voltage of U_2 in the reverse-bias direction.

EVALUATION

If a module only supplies half the amount of photoelectric current, for example, it will be responsible for determining the short-circuit current for the whole series circuit in the absence of any by-pass diodes.

With by-pass diodes, the fully illuminated module can supply its higher current until this starts to decrease when the open-circuit voltage of the individual module is reached.

The mathematical model for evaluating the measurements in Figs. 3 and 4 takes into account Kirchhoff's laws and utilises the current-voltage characteristic for the individual modules obtained in Experiment UE8020100 with parameters I_s , U_T and R_p . To take account of the by-pass diodes, their own characteristics are used.

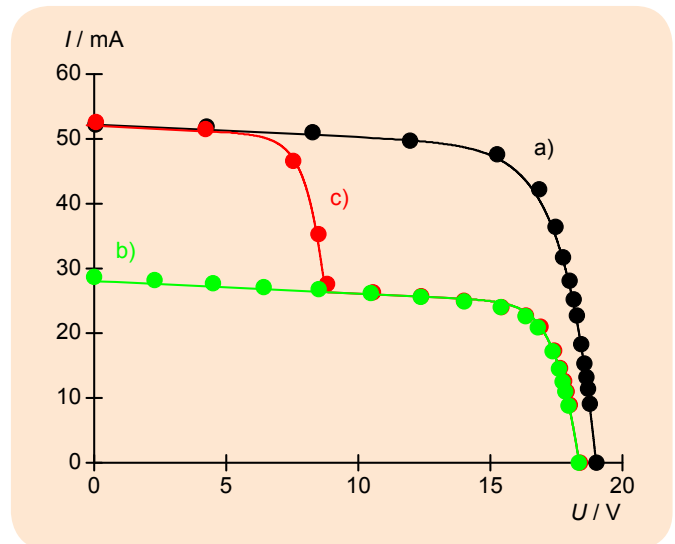


Fig. 3: I - U characteristic for series circuit containing two solar modules a) with no shading, b) partial shading without by-pass, c) partial shading with by-pass

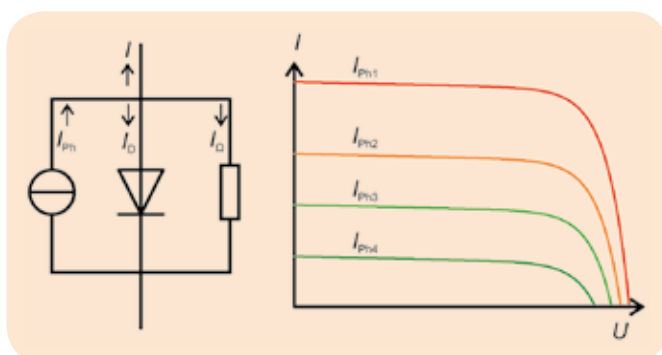


Fig. 1: Equivalent circuit diagram and characteristics of a solar cell

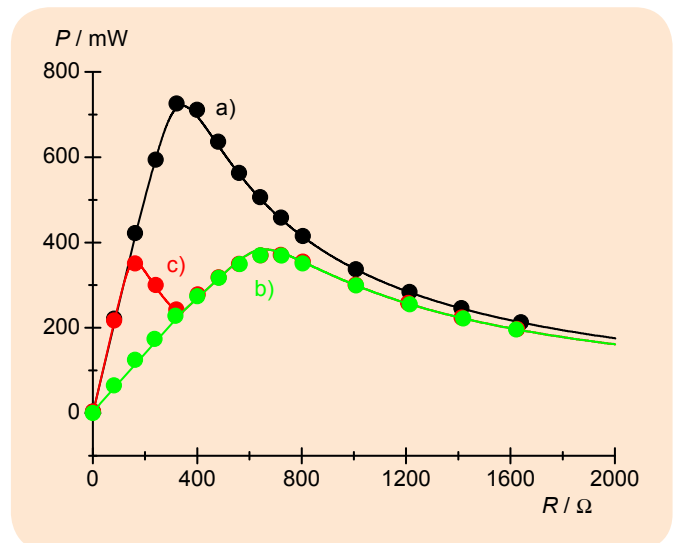
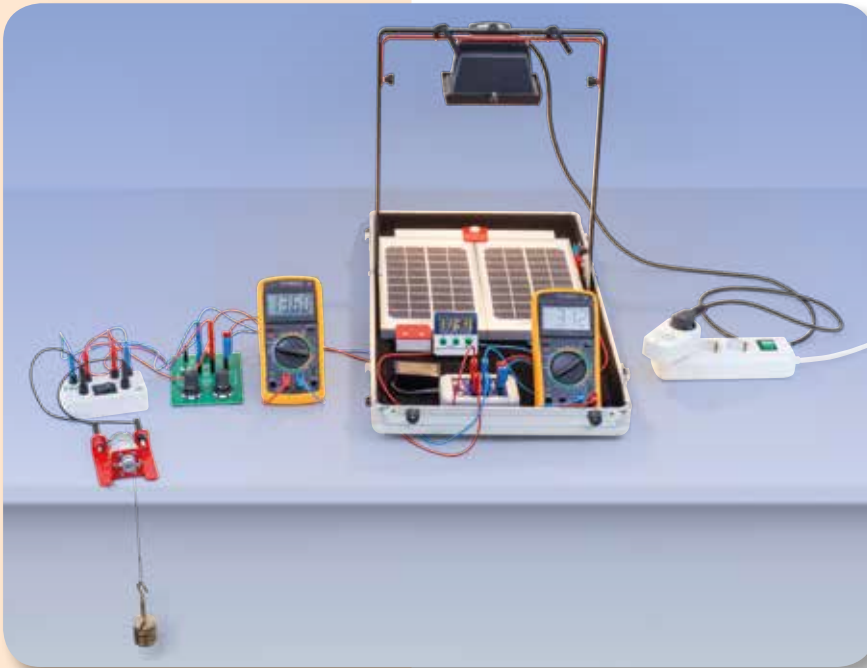


Fig. 4: P - R characteristic for series circuit containing two solar modules a) with no shading, b) partial shading without by-pass, c) partial shading with by-pass

UE8020250

PHOTOVOLTAIC SYSTEMS



OBJECTIVE

Investigation of an island grid or micro-grid used to generate and store electrical energy

EXPERIMENT PROCEDURE

- Determining the operating current of the electronic charge meter and the minimum illuminance required for operation.
- Investigating the current balance of the island grid for various resistive loads and different luminosities in lab operation.
- Measuring the solar power being delivered and the charging or discharging current as a function of the load current for different illuminance levels.



You can find technical information about the equipment at 3bscientific.com

1

SUMMARY

Island grids or microgrids are power supply systems without any connection to a public utility grid and incorporate both generation and storage of electrical energy. Frequently photovoltaic modules are used to generate power and accumulators are used for energy storage. In order to simulate such an island grid in an experiment, two photovoltaic modules are used to charge up a nickel-metal hydride battery. A DC motor is deployed as the connected load which discharges the accumulator, while an electronic charge meter measures the electrical charging and discharging of the battery. Thanks to a series connection of the two modules a reliable charging of the accumulator is achieved also when there is less illuminance, since idle voltage is still far above the accumulator voltage level.

REQUIRED APPARATUS

Quantity	Description	Number
1	SEK Solar Energy (230 V, 50/60 Hz)	1017732 or
	SEK Solar Energy (115 V, 50/60 Hz)	1017731
1	Coulombmeter with Rechargeable Battery	1017734
1	Geared Motor with Pulley	1017735
1	Set of Slotted Weights, 5 x 50 g	1018597
1	Cord, 100 m	1007112
1	Two-pole Switch	1018439
1	Set of 15 Experiment Leads, 75 cm 1 mm ²	1002840
1	Timer	1003009

BASIC PRINCIPLES

Island grids are off-grid power supply systems without a connection to a public utility grid. They include power generation and storage and are normally deployed when connection to the public utility grid is either impossible or inefficient, or when this offers insufficient flexibility and mobility. Photovoltaic modules are frequently used to generate power and accumulators for storing energy in this context. To emulate this kind of off-grid island system two photovoltaic modules are used in the experiment, each having a nominal power of 5 W for charging a nickel-metal

hydride battery with a capacitance of 220 mAh. A DC motor functions as a connected load discharging the accumulator while an electronic charge meter is used to measure current charging and discharging. We dispense with the charge controller usually deployed in this context.

The voltage U_{Accu} of the accumulator has a nominal rating of 8.4 V, but depends on the charging state as well as the charge current I_{Accu} and conventionally reaches up to 10 V. It determines the voltage in all circuit branches connected in parallel (see Fig. 1):

$$(1) \quad U_{Accu} = U_{Op} = U_L = U_{Solar}$$

The current supplied I_{Solar} is used as the basic operating current I_{Op} for the electronic charge meter, as charging current I_{Accu} for the accumulator and as current I_L flowing through the connected resistive load. The electric balance

$$(2) \quad I_{Solar} = I_{Accu} + I_{Op} + I_L$$

This also applies for cases of negative charge current I_{Accu} , i.e. in cases where the accumulator is discharging power.

The operating current $I_{Op} = 10$ mA is defined by the electronic circuit of the charge meter, while the load current I_L depends on the ohmic resistance R_L of the connected load. The accumulator is thus charged up when the photovoltaic system supplies power and the load resistance is not too low. To ensure reliable charging of the accumulator during lower illuminance levels, it is important to configure the photovoltaic system so that its idle voltage U_{OC} is significantly higher than the voltage U_{Accu} . A comparison with the characteristics measured in the experiment UE8020100 shows that this can be reasonably reached by connecting the two modules in series configuration. Then the solar power supplied I_{Solar} is, in good approximation, proportional to the luminosity E and under laboratory conditions reaches values up to 50 mA, which are optimal for rapid charging of the accumulator.

A DC motor and a cascade resistor configuration are used as resistive loads with which the charging current/load current characteristics of the island grid is sampled and furthermore verified that the solar current supplied is independent of the resistive load. In the results the minimum brightness can be specified, for example, which is needed to charge the accumulator in the absence of all loads.

NOTE

When operating the photovoltaic module in sunlight outdoors, considerably higher electrical currents are reached. Here the accumulator should not be connected without additional resistive load which should ensure that the charging current does not exceed $I_{Accu} = 44$ mA.

EVALUATION

The operating current of the charging meter is determined from the charge flowing in 30 s out of the accumulator, if neither module nor load are connected.

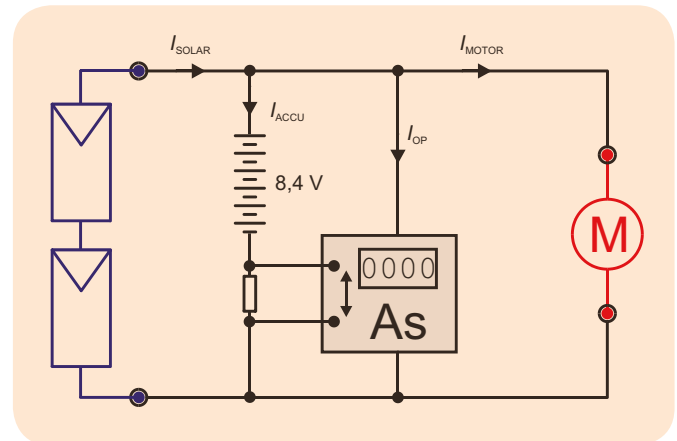


Fig. 1: Block circuit diagram of island grid

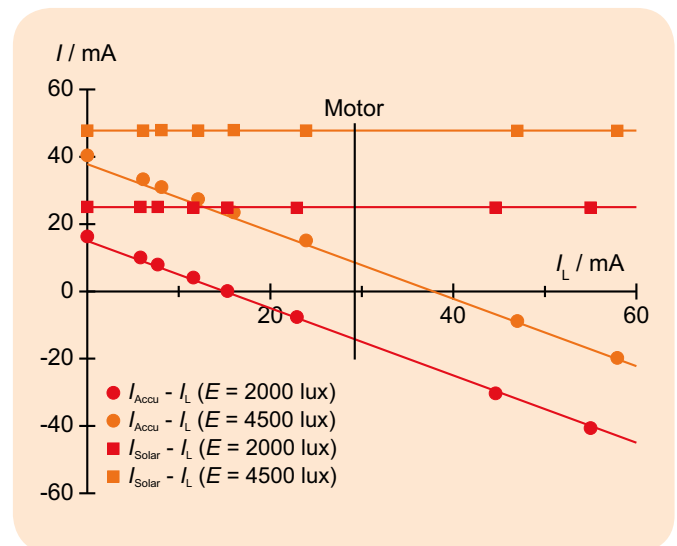


Fig. 2: Load characteristics of island grid

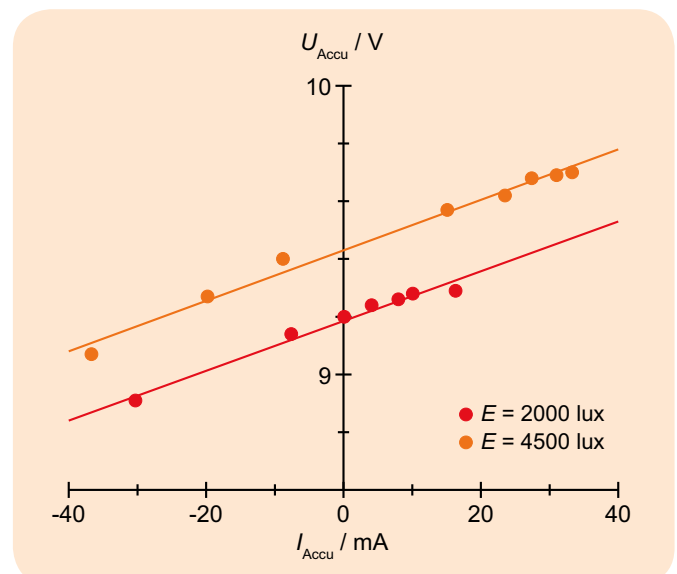
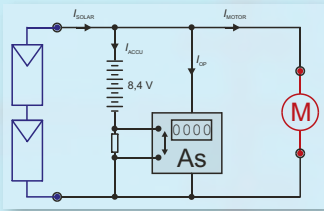
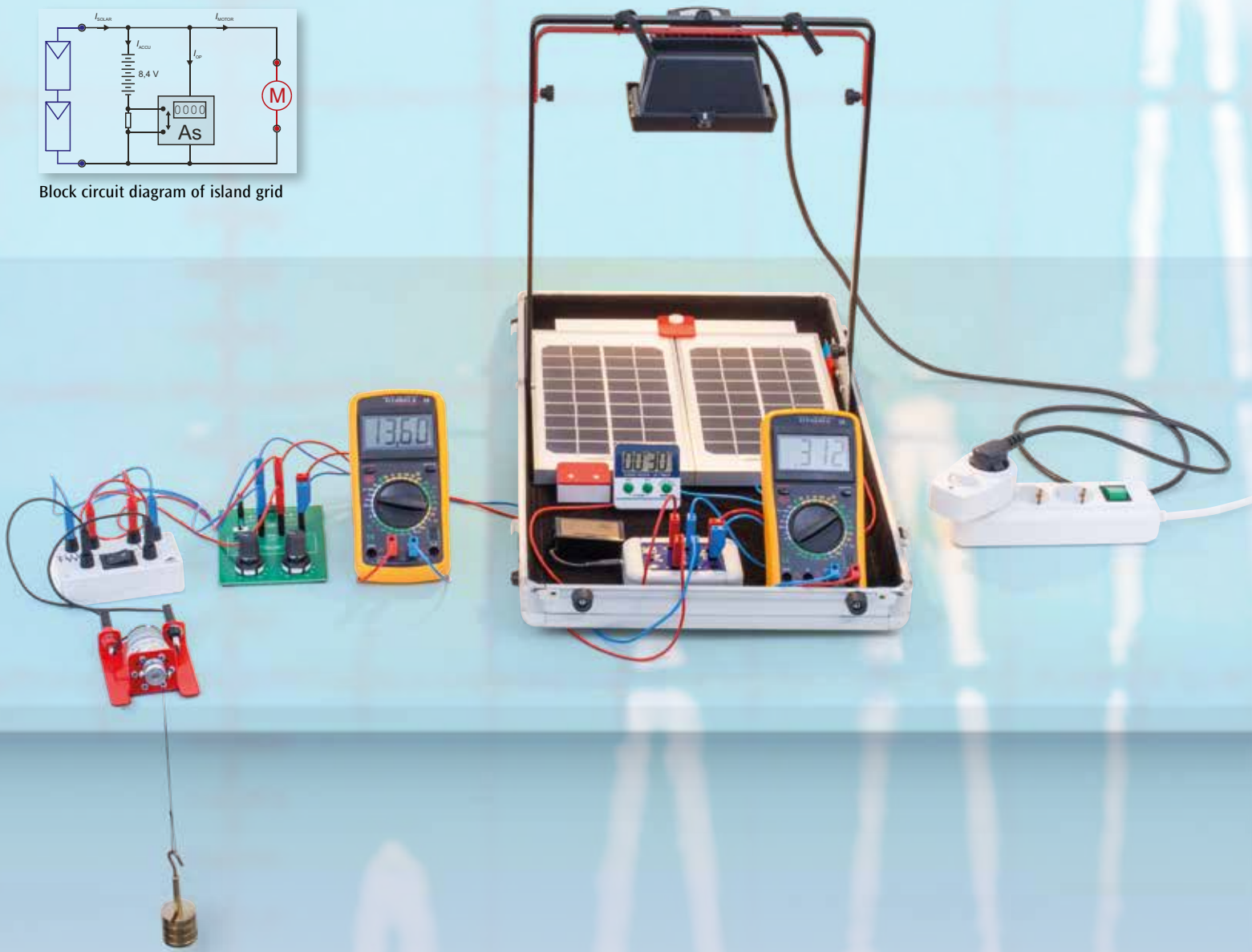


Fig. 3: Characteristics of the accumulator, measured at different luminosities. Depending on the accumulator's charging state, these characteristics are shifted up or down on the y-axis.



Block circuit diagram of island grid



Photovoltaic systems (UE8020250):

Investigation of an island grid or microgrid used to generate and store electrical energy

Island grids or microgrids are power supply systems without any connection to a public utility grid and incorporate both generation and storage of electrical energy. Frequently photovoltaic modules are used to generate power and accumulators are used for energy storage. In order to simulate such an island grid in an experiment, two photovoltaic modules are used to charge up a nickel-metal hydride battery. A DC motor is deployed as the connected load which discharges the accumulator, while an electronic charge meter measures the electrical charging and discharging of the battery. Thanks to a series connection of the two modules a reliable charging of the accumulator is achieved also when there is less illuminance, since idle voltage is still far above the accumulator voltage level.